MICROREVIEW

# Organic and organometallic fluorinated materials for electronics and optoelectronics: a survey on recent research

Roberta Ragni,[a] Angela Punzi,[a] Francesco Babudri*[a] and Gianluca Maria Farinola*[a]

Dedication ((optional))

**Abstract**: Conjugated organic polymers, small molecules and transition metal organometallic complexes are used as active semiconducting materials in electronic and optoelectronic devices including Organic Solar Cells (OSCs), Organic Field Effect Transistors (OFETS), Organic Light Emitting Diodes (OLEDs). While some of these technologies are mature and already available on the market, research is still very active in academic and industrial laboratories to gain better performances. Major drawbacks which still limit large industrial production of some of these devices are not only the non-optimized performances, but also stability issues and cost. In fact, wide applicability of organic electronic technology largely relies on the development of efficient, durable and cost-effective materials. Properties of molecular and polymeric semiconductors can be properly engineered and finely tuned by the design of the conjugated molecular structure and the selective introduction of various functional groups as the substituents. Selective functionalization of the conjugated backbone with fluorine atoms and fluorinated substituents has been largely demonstrated to be an effective structural modification not only for tuning optoelectronic properties, but also to affect solid state organization and to improve stability. This review covers the most important classes of materials (conjugated polymers, small molecules and organometallic complexes) reporting for each of these classes the applications in OSCs, OFETs and OLEDs and highlighting the role of fluorine functionalization on the properties. The literature shows intriguing results that can be achieved by fluorine functionalization, and it also points out that this research field is still promising for future progresses.

## 1. Introduction

The concept of “plastic electronics” was originated by the discovery of the semiconducting behavior in some classes of organic materials and by their suitability for fabrication of electronic and optoelectronic devices. For most of organic semiconducting materials, solution processing techniques are available, also for large area devices, and they are relatively inexpensive if compared to high-temperature processing generally required for inorganic semiconductors. Moreover, fabrication of flexible, plastic, large area electronic devices opens up unconventional technological solutions for consumable and disposable electronics. The major drawback of the organic-based electronics consists in lower performances with respect to their inorganic counterparts. However, recent progresses in materials’ design and synthesis are reducing this gap and, up today, several electronic devices such as Organic Solar Cells (OSCs), Organic Field Effect Transistors (OFETS) and Organic Light Emitting Diodes (OLEDs) have reached prominent levels of efficiency, comparable to those of the analogous inorganic devices. Conjugated polymers, oligomers, small molecules and transition metal organocomplexes are promising organic semiconductors, whose electronic and optical properties can be modulated by properly engineering the conjugated molecular structure and its functionalization. On this ground, fluorine atom is one of the most attractive substituents: it is a strong inductive electron-withdrawing atom that also plays an effective resonance electron-donating effect. These features affect both the HOMO and LUMO energy levels in a conjugated system, generally lowering the HOMO energy with minor effect on the LUMO. Consequently, a widening of the band-gap may result by introduction of fluorine as substituent in a conjugated chain. In addition to electronic effects, several non-covalent interactions of fluorine with hydrogen, sulfur and halogen atoms and $\pi$–orbitals, combined with the small dimension of the fluorine atom (only 20% larger than hydrogen), may significantly influence the molecular organization in the solid state by promoting planarization of the conjugated backbone and improving the $\pi$–$\pi$ stacking and charge carrier transport across the semiconducting material. OSCs, OFETs and OLEDs performances can be markedly modified by these effects.

In 2007 we published a concise review on fluorinated organic materials for electronic and optoelectronic applications.[1] Dating this time, an impressive variety of fluorine functionalized organic semiconductors has been produced and applied in devices.

In our work on conjugated materials synthesis and applications,[2] fluorine derivatives played a relevant role and the interest for their singular properties is the ground of this short account. This survey is not meant to be an exhaustive review on the subject, but rather a critical collection of more recent significant examples, highlighting the potentialities but also the drawbacks of introducing fluorine atoms in the conjugated skeletons of the major typologies of organic semiconductors. This review is organized in different sections focused on electronic device typology (OSCs, OFETs and OLEDs) and, for each of them, the role of fluorination is analyzed for polymers, small molecules and organometallic complexes.

## 2. Organic electronic devices: characteristics.

Fluorination of organic and organometallic compounds significantly influences the photophysical properties of these materials and their performances in devices. The approach to fluorination of organic and organometallic compounds significantly influences the photophysical properties of these materials and their performances in devices.

[a] Dipartimento di Chimica
Università degli Studi di Bari Aldo Moro
via Orabona, 4 70125 Bari (Italy)
E-mail: francesco.babudri@uniba.it; gianlucamaria.farinola@uniba.it

**Roberta Ragni** graduated in Chemistry in 2001 and received her Ph.D. degree in Chemical Sciences at the University of Bari, Italy, in 2004. In 2006, she was a visiting researcher at the Instituut voor Moleculaire Chemie-Universiteit van Amsterdam, The Netherlands, and at the Westfälische Wilhelms-Universität Münster Physikalisches Institut, Germany. She has held a position as Researcher in Organic Chemistry at the University of Bari since 2008. Her research interests deal with the synthesis and properties of (electro)-luminescent organic and organometallic compounds, and biohybrid materials for photonics, biomedicine, and solar-energy conversion.

**Angela Punzi** graduated in Chemistry at the University of Bari in 1990. Currently, she is Assistant Professor at the Chemistry Department of the same University. Her research interests focus on the synthesis of π-conjugated compounds, such as stereodefined polyenes, aromatic heterocycles and molecular or polymeric materials for both biological and optoelectronic applications, by organometallic-based and/or direct arylation protocols.

**Francesco Babudri** was born in Bari (Italy) in 1953 and received his "Laurea" in Chemistry from the University of Bari in 1976. He started his career as Researcher in 1978 at the Department of Chemistry of the same University, working with Professor S. Florio in the field of organometallic chemistry. After a stay at the "Laboratoire de Chimie" of the "Ecole Normale Superieure" in Paris (1988) with Professor P. Sinaÿ, he joined the research group of Professor F. Naso at the University of Bari, working in the field of organometallic chemistry applied to the synthesis of polyunsaturated compounds. Currently, he is Professor of Organic Chemistry at the same University. His main research interests focus on polymer chemistry, materials, and synthetic strategies.

**Gianluca M. Farinola** received his Ph.D.degree in Chemical Sciences in 1997 and is a Full Professor of Organic Chemistry at the University of Bari “Aldo Moro.” He is presently in charge as the President of the Organic Chemistry Division of the Italian Chemical Society (2017–2019). He has been a visiting professor at the Universities of Muenster (2009), Strasbourg (2013–2014), Angers (2015), and Tufts in Boston (2017). His research activity focuses on synthetic routes to organic, organometallic, and biohybrid materials for optoelectronics and biology.

The approach to organic fluorinated semiconductors adopted in this review is focused on the comparison of the performances of these materials with respect to their non-fluorinated analogues. Hence, the evaluation of the effects of fluorine substituents requires the analysis of physical and electrical parameters that are peculiar for OSCs, OFETs and OLEDs. For better comprehension of the review by a broad readership, here we summarize these parameters, that are discussed more in detail in the literature for organic electronics and optoelectronics.[3]

Organic solar cells

The efficiency of conversion of solar energy in electric power (PCE) is defined by the following formula:

$$PCE = \frac{V_{oc} * J_{sc} * FF}{P_{in}}$$

where: $V_{oc}$ (open circuit voltage) represents the maximum output voltage that the cell is able to generate under illumination at zero current flowing in the cell;

$J_{sc}$ is the highest density current flowing in the cell when no external field is applied and charges are drifting by effect of internal field;

FF (Fill Factor) evaluates the loss of charge carriers by recombination process and it is determined by photo-generated charges that reach electrodes;

$P_{in}$ is the power of the incident light standardized to 1000 $Wm^{-2}$ with a spectral intensity distribution matching the sun power that reaches the earth surface at an incident angle of 48.2°.

Moreover, the external quantum efficiency (EQE) of a OSC is the ratio of the electrons collected in short circuit conditions to the incident photons at specified wavelength.

Organic Field Effect Transistors

The evaluation of the performances of organic semiconductors in OFETs is based on two parameters. The charge mobility ($\mu$ [$cm^2 V^{-1}s^{-1}$]) measures the ability of charge carriers (electrons or holes) to drift through the semiconductor under an applied electric field. Typical charge mobilities in OFETs range from 0.01 to over 1$cm^2 V^{-1} s^{-1}$ for high speed digital circuits. The $I_{on}/I_{off}$ current ratio is the ratio of the current flowing between the source and drain electrodes when the device is in the on state and the same current in the off state. It depends on several parameters such as the charge injection efficiency from electrodes, semiconductor purity and morphology of the thin film. Large values over $10^6$ are required for efficient OFETs.

Organic Light Emitting Diodes

The internal quantum efficiency ($\eta_{int}$) of OLEDs is the ratio of the total number of photons generated within the device to the number of electron injected. However, for display applications, the external quantum efficiency ($\eta_{ext}$), defined as the ratio of the number of photons emitted in the viewing direction to the number of electrons injected, is more frequently used. The external and internal efficiencies differ by the fraction of light that is dispersed out the viewing direction and $\eta_{int}$ can be several times higher than $\eta_{ext}$. The luminous efficiency $\eta_l$ ($cdA^{-1}$) is defined as:

$$\eta_l = \frac{A * L}{I}$$

where A is the active area of device, L is the luminance ($cdm^{-2}$) and I is the current flowing in the device. This parameter weights all incident photons according to the phototopic response of eye, this meaning that photons emitted out the range of visible light do not contribute to $\eta_l$. Power efficiency or luminosity ($\eta_p$ lm $W^{-1}$) is the ratio of luminous power (lm) emitted in forward direction to the electrical power required to drive the OLED at specified voltage. For example $\eta_p$ is about 20 lm $W^{-1}$ for incandescent light bulb and reach 50-100 lm $W^{-1}$ for a fluorescent bulb.

## 3. Organic fluorinated materials for photovoltaics

### 3.1. Conjugated polymers

The introduction of the bulk heterojunction concept (BHJ) in 1995[4] has boosted the interest towards OSCs as substitutes or integration of conventional silicon-based photovoltaics. Among the organic materials that show great potentialities in OSCs, conjugated polymers have attracted the major interest. Low band-gap copolymers, alternating in their structure electron-rich (donor, D) and electron-poor (acceptor, A) units, often joined by π-conjugation bridge (thiophene or benzene units), turned out to be useful donor materials owing to the possibility of fine tuning the HOMO and LUMO levels to obtain the best matching with those of the most used fullerene-based ($C_{61}$ and $C_{71}$) acceptors.[5] The introduction of fluorine atoms as substituents on the copolymer chains was proven to be an effective strategy to lower the HOMO energy level achieving higher open-circuit voltage ($V_{oc}$) and better power conversion efficiency (PCE) versus their non-fluorinated counterparts ("F effect"). Moreover, the presence of fluorine atoms has a strong impact on the morphology of the active layer by increasing the planarity of conjugated systems and modifying their miscibility with fullerene acceptors. The resulting reduced crystalline domain size, the enhanced structural order and better face-on polymer orientation at the polymer-fullerene or at the polymer/electrode interfaces generally improve the device performances. Recently, non-fullerene small molecules have been introduced as effective electron acceptor substitutes of fullerene derivatives. A device with 13.1% PCE was obtained introducing fluorine atoms on both the donor polymer and the non-fullerene acceptor.

Most significant results obtained by the fluorination strategy in polymer-based OSCs have been recently reviewed.[6] In this section we report some selected recent results not covered in the above quoted review. In Chart 1, some examples of the most performing D-A (or D-π-A) polymers are shown and compared with their non-fluorinated counterparts. Data on related OSCs are reported in Table 1.

The benzodithiophene is the most common donor unit in D-A copolymers in combination with several acceptor units such as benzothiadiazole and benzotriazole. In these polymers the effect of fluorine atoms on the donor or on the acceptor units has been investigated. Fluorine atoms in the benzothiadiazole units of PF1, PF2,[7] P2 and P3[8] polymers improve the devices PCE with respect to the non-fluorinated PF0 and P1, when $PC_{71}BM$ is used as the acceptor (Chart 1). Fluorination mainly lowers the HOMO energy level, thus increasing the $V_{oc}$. In the case of P3, the effect of molecular weight was also studied, evaluating the performances of three samples with $M_w$ 90.2 (low MW P3), 159.5 (medium MW P3) and 215.2 (high MW P3) KDa. The increase of PCE from low MW P3 to medium MW P3 is mainly due to the increase of short-circuit density current ($J_{sc}$= 12.7 and 14.1 mA $cm^{-2}$, respectively). Conversely, $J_{sc}$ decreases for the high MW P3-based device ($J_{sc}$ = 11.7 mA $cm^{-2}$). This rather unexpected result is ascribed to a lower solubility of high MW P3 in *o*-dichlorobenzene used in the film deposition, causing unfavourable blend morphology. For medium MW P3 the use of 1,8-diodooctane as additive increases further both $J_{sc}$ and fill factor (FF) resulting in a better PCE.

In HTAZ polymer,[9] fluorine atoms were introduced on acceptor unit (FTAZ), in the 3' or 4' positions of the thiophene units (3'-FT-HTAZ and 4'-FT-HTAZ) and in both ring systems (3'-FT-FTAZ and 4'FT-FTAZ). This investigation highlights that the position of fluorine atoms in the conjugated backbone can play a crucial role. In some cases, it can also negatively affect the performances of photovoltaic devices. The introduction of fluorine atoms on the benzotriazole units lowers, as expected, the HOMO level of FTAZ. The resulting increase of $V_{oc}$ is the main factor enhancing the PCE in $PC_{61}BM$-based optimized devices with respect to those made with HTAZ. The energy of HOMO level does not change significantly by shifting the fluorine atoms from the benzotriazole unit to the 3' or 4'-position of thiophene rings in 3'-FT-HTAZ and 4'-FT-HTAZ or in tetrafluorinated 4'-FT-FTAZ. These results suggest that the "F effect" can be maintained, independently on the position of the fluorine on the acceptor or donor units in DA polymers. An unexpected fall of PCE is evidenced for 3'-FT-FTAZ, due to a dramatic drop of $J_{sc}$. DFT calculation and $^1H$ and $^{19}F$NMR spectral evidences on 3'-FT-HTAZ and 3'- FT-FTAZ allow to conclude that, in their preferred conformation, fluorine substituents on thiophene units flank hydrogen (in 3'-FT-HTAZ) or fluorine (in 3'-FT-FTAZ) atoms of the benzotriazole unit (Fig. 1). The interaction H-F does not cause a significant distortion from planarity of the conjugated backbone, that, on the contrary, is much greater in the case of the F-F one. The resulting reduced conjugation extent increases the band-gap value of the 3'-FT-FTAZ and reduces the hole mobility and, in turn, the $J_{sc}$.

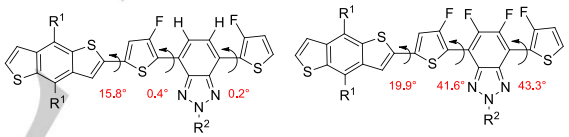


**Figure 1.** Distortion from planarity in 3'-FT-HTAZ and 3'-FT-FTAZ polymers

The performances of FTAZ can be further improved in devices with inverted configuration by using ITIC (Fig. 2), a non fullerene acceptor.[10]

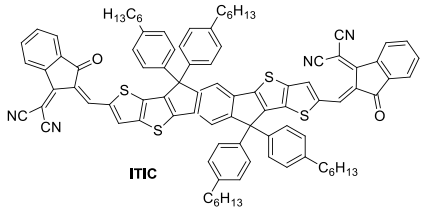


**Figure 2.** ITIC non fullerene acceptor

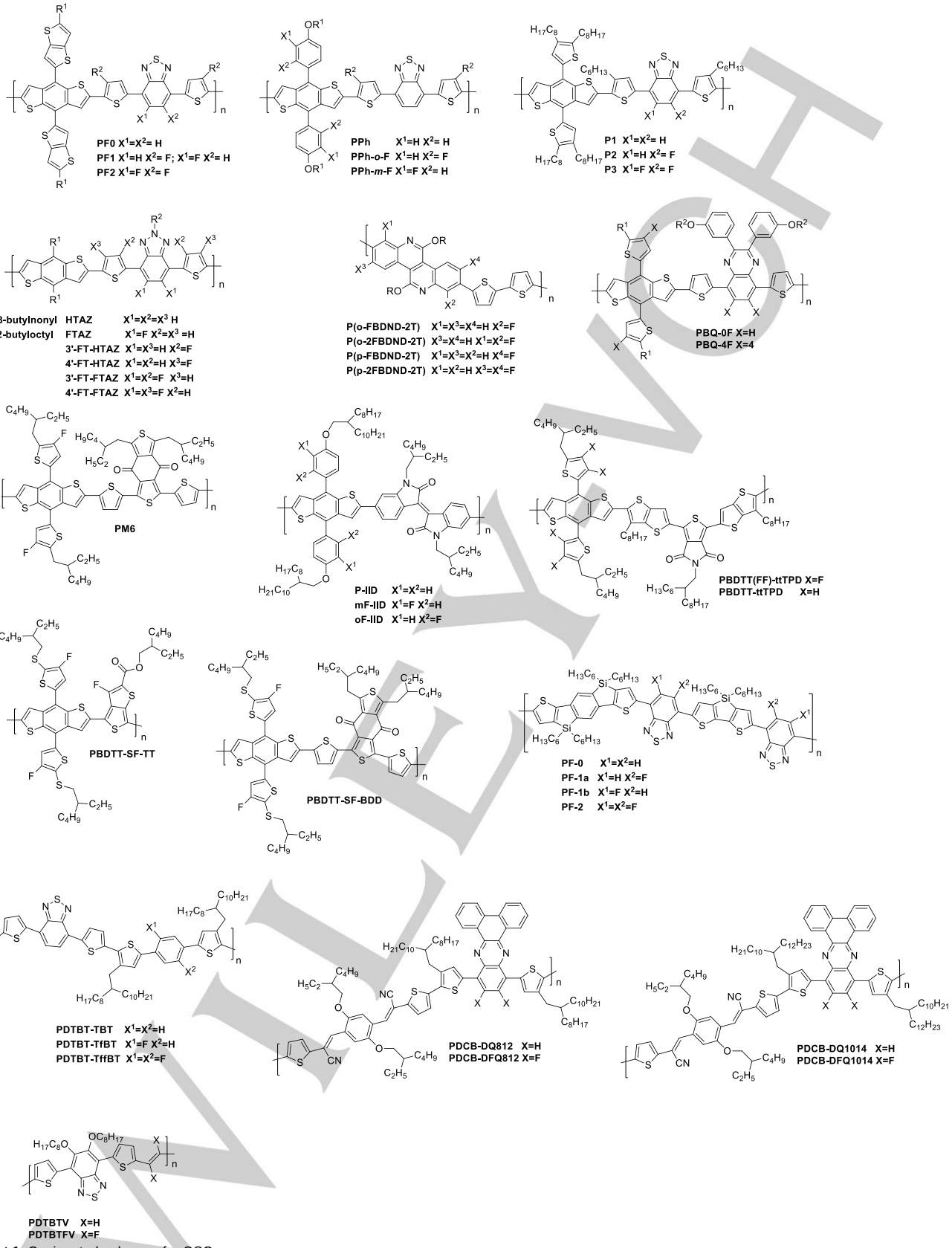


**Chart 1.** Conjugated polymers for OSCs

**Table 1.** Characteristic parameters for OSCs made with polymers in Chart 1

| *Polymer* | *PCE (%)* | *$V_{oc}$(V)* | *$J_{sc}$(mA cm$^{-2}$)* | *FF (%)* |
|---|---|---|---|---|

| | | | | |
|---|---|---|---|---|
| PF0 | 5.70 | 0.74 | 11.76 | 65.46 |
| PF1 | 6.29 | 0.80 | 11.85 | 66.23 |
| PF2 | 6.54 | 0.86 | 11.67 | 65.25 |
| PPh | 6.23 | 0.83 | 11.33 | 66.3 |
| PPh-m-F | 6.62 | 0.91 | 11.25 | 64.6 |
| PPh-o-F | 2.51 | 0.96 | 4.31 | 60.6 |
| P1 | 6.07 | 0.75 | 11.7 | 69.2 |
| P2 | 6.33 | 0.79 | 11.6 | 69.1 |
| P3 low MW | 7.48 | 0.85 | 12.7 | 69.3 |
| P3 medium MW | 8.16 (8.47)[a] | 0.85 (0.80)[a] | 14.1(14.8)[a] | 68.1 (71.5)[a] |
| P3 high MW | 6.26 | 0.82 | 11.7 | 71.5 |
| HTAZ | 4.39 (4.26)[b] | 0.74 (0.85)[b] | 11.10 (12.54)[b] | 53.3 (39.9)[b] |
| FTAZ | 6.58 (8.37)[b] | 0.81 (0.91)[b] | 12.02 (16.25)[b] | 68.0 (56.5)[b] |
| 3'FT-HFTAZ | 7.42 | 0.91 | 11.72 | 69.6 |
| 4'FT-HFTAZ | 6.82 | 0.82 | 12.02 | 69.3 |
| 3'FT-FTAZ | 3.05 | 0.99 | 6.01 | 51.2 |
| 4'FT-FTAZ | 7.74 | 0.92 | 12.39 | 67.8 |
| P(o-FDBND-2T) | 1.44 | 0.87 | 2.63 | 62.0 |
| P(o-2FDBND-2T) | 0.79 | 0.89 | 1.50 | 56.0 |
| P(p-FDBND-2T) | 6.55 | 0.89 | 10.12 | 66.0 |
| P(p-2FDBND-2T) | 5.27 | 0.90 | 7.86 | 67.0 |
| PBQ-0F[c] | 5.40 | 0.66 | 11.82 | 69.2 |
| PBQ-4F[c] | 8.18 | 0.88 | 13.26 | 70.1 |
| PBQ-0F[d] | 5.32 | 0.65 | 11.98 | 70.1 |
| PBQ-4F[d] | 9.04 | 0.89 | 14.43 | 70.4 |
| PM6[b] | 9.70 | 1.04 | 16.0 | 58.0 |
| P-IID | 5.23 | 0.84 | 9.68 | 64.3 |
| mF-IID | 2.50 | 0.88 | 5.61 | 50.5 |
| oF-IID | 0.93 | 0.96 | 1.61 | 60.2 |
| PBDTT(FF)-ttTPD | 7.45 | 0.98 | 12.49 | 61.0 |
| PBDTT-ttTPD | 6.79 | 0.84 | 12.07 | 67.0 |
| PBDTT-SF-TT | 9.07 | 1.00 | 14.79 | 61.1 |
| PBDTT-SF-BDD | 9.72 | 0.97 | 14.70 | 67.5 |
| PF-0 | 5.58 | 0.68 | 14.06 | 58.4 |
| PF-1a | 7.02 | 0.74 | 15.99 | 59.3 |
| PF-1b | 8.00 (8.42)[e] | 0.74 (0.76) [e] | 17.02 (17.20) [e] | 63.3 (64.5) [e] |
| PF-2 | 7.08 | 0.82 | 14.05 | 61.3 |
| PDTBT-TBT | 5.84 | 0.77 | 11.50 | 66.0 |
| PDTBT-TfBT | 5.44 | 0.81 | 9.61 | 70.0 |
| PDTBT-TffBT | 7.53 | 0.79 | 13.44 | 71.0 |
| PDCB-Q812[b] | 5.19 | 0.89 | 10.90 | 53.3 |
| PDCB-DFQ812[b] | 8.17 | 1.03 | 13.44 | 58.9 |
| PDCB-Q1014[b] | 3.26 | 0.89 | 7.98 | 45.8 |
| PDCB-DF1014[b] | 7.08 | 1.04 | 10.89 | 62.3 |
| PDTBTV | 0.53 | 0.55 | 3.33 | 28.3 |
| PDTBTFV | 1.24 | 0.83 | 4.32 | 34.6 |

[a]Device with 3% of 1,8-diiodooctane;[b]Device with ITIC as the electron acceptor; [c]Ca/Al cathode; [d]PFNBr/Al cathode; [e]device with inverted configuration.

In this case, the improved performances of FTAZ:ITIC with respect to HTAZ:ITIC are mainly due to an increase of the $J_{sc}$ value, that was not evidenced in the previous devices with fullerene acceptor. Better performances of FTAZ:ITIC devices may be explained on the basis of improved charge transport and extraction due to higher hole and electron mobilities in the fluorinated polymer.

An adverse "F Effect" due to fluorine position is also found in dibenzonaphtyridinedione P(o-FBDND-2T) and P(o-2FBDND-2T) polymers,[11] bearing one or two fluorine atoms in the "ortho" (with respect to the heterocycle nitrogen atoms) positions, respectively. These copolymers show poorer performances in OSCs with $PC_{71}CM$ fullerene acceptor versus their "para" isomers. Also in this case, the marked differences in PCE are related to the lower $J_{sc}$ in the "ortho" isomer-based devices, the $V_{oc}$ and FF being almost unaltered. The low $J_{sc}$ is directly related to reduced hole mobility in films. In the "ortho" isomers weaker intermolecular interactions increase the solubility of the polymer in *o*-DCB and lead to the formation of large polymer domains in the film, which negatively affect the exciton separation. The "para" isomers, owing to stronger intermolecular interactions, show poorer solubility and form smaller nanowire-like fibril networks that facilitate the charge separation of excitons.

In PDTBT-TBT,[12] fluorine atoms are present in the benzene ring of the dithiophene-benzene-dithiophene donor moiety, the benzothiadiazole system being the acceptor unit. Both PDTBT-TfBT and PDTBT-TffBT show almost the same $V_{oc}$ values, which are higher than PDTBT-TBT in devices with $PC_{71}BM$. However, PCE of PDTBT-TfBT-based OSC is noticeably lower than PDTBT-TBT-based devises, due to decreased $J_{sc}$. DFT calculations and spectroscopic investigations emphasize that thiophene-benzene-thiophene segment of the polymer suffers from greater distortion from planarity in PDTBT-TfBT when single fluorine atom is present on the phenyl ring. On the contrary, the same moiety of the conjugated chain is nearly planar in PDTBT-TffBT. The reduced planarity of PDTBT-TfBT, that prevents strong intermolecular interaction, reduces conjugation length with detrimental effects on the charge carrier mobilities and, consequently, on the $J_{sc}$ value.

The PF polymers[13] (PF-0, PF-1a, PF-1b, PF-2) are characterized by a D-A-D'-A structure with two different donor units both containing silole functionalities. The presence of two different donor units generates PF-1a and PF-1b regioisomercopolymers by monofluorination on the benzothiadiazole ring of PF-0. OSCs made with these polymers and $PC_{71}BM$ show different behavior, the higher PCE being obtained from PF-1b (8.00% versus 7.02% for PF-1a) that is further increased (8.42%) adopting the inverted device structure. Also in this case, the higher value of $J_{sc}$ is the origin of better performances of PF-1b, whose increase is ascribed to a more ordered solid structure, evidenced by GIWAXS and AFM investigations, that enhances intermolecular contacts and improves charge transport.

PDCB-DQ812 and PDCB-DQ1014 polymers[14] show both quinoxaline and cyanostyrylbenzene units as acceptor moieties. Quinoxaline bears two phenyl substituents in 2 and 3 positions that are bound together by a single bond between the ortho positions; this structural feature increases the planarity of the conjugated chain and facilitates the intermolecular packing and charge transport. On the other hand, the cyano group has a beneficial effect on charge mobility by increasing the electron affinity. The HOMO/LUMO levels of these polymers match well those of ITIC and fair PCEs for devices made with this non-fullerene acceptor and PDCB-DQ812 are reported. For PDCB-DQ1014, PCE is significantly lower. The presence of two different alkyl chains on PDCB-DQ812 and PDCB-DQ1014 does not influence the HOMO/LUMO levels. However, PDCB-DQ1014 has lower extinction coefficient and $J_{sc}$ measured in the device with respect to PDCB-DQ812, this likely explaining its poorer performances. The introduction of fluorine atoms on the residual free positions of the quinoxaline system has no effect on the LUMO levels of PDCB-DFQ812 and PDCB-DFQ1014, but the HOMO levels are lowered, thus enhancing not only the $V_{oc}$ but also $J_{sc}$ and FF, so that increasing the PCEs.

Other examples of vinylene polymers are PDTBTV and PDTBFV bearing benzothiadiazole as acceptor units and fluorine atoms on

the vinylene unit.[15] The higher PCE of PDTBFV-based OSC (1.24%) with respect to the non-fluorinated one (0.46%) is again due to an increase of both $V_{oc}$ and $J_{sc}$. Fluorine atoms on the double bonds act on the frontier molecular orbitals by lowering the HOMO level, and also increase the extinction coefficient by favoring planarization of the conjugated chains and promoting intermolecular interactions. All these combined features allow to reduce the BHJ film thickness and enhance the charge carrier generation at the polymer-acceptor interface and their collection at the electrodes.

The presence of a pendant conjugated chain in D-A copolymer, mainly with benzodithiophene as donor unit, is reported to be an effective means for controlling energy levels, absorption properties and charge transport. Although thiophene based pendant chains are most common, phenyl units are more effective in increasing $V_{oc}$ and improving intermolecular packing and charge transport, with positive effects on $J_{sc}$. Several studies are reported in the literature about the effectiveness of fluorination of side chains in DA copolymers but, as previously discussed for fluorine atoms in the main chain, the positive "F-effect" is strongly dependent on the position of halogen atoms. Poorer performances have been reported for PPh-o-F polymer with respect to the meta PPh-m-F isomer and the non-fluorinated PPh polymer.[16] Also in this case, the PCE values of devices with $PC_{71}BM$ are influenced mainly by the $J_{sc}$, although the $V_{oc}$ values increase from PPh to PPh-o-F and PPh-m-F, according to the lowering of their HOMO energy levels. The fluorine atom in the orto position increases the distortion angle between the pendant phenyl groups and the benzodithiophene ring. Therefore, conjugation length and intermolecular packing are reduced with a detrimental effect on the efficiency of charge transport. Similar results are reported for mF-IID and oF-IID copolymers with respect to the parent P-IID.[17] The presence of fluorine atoms both on orto and meta positions of the phenyl rings of the pendant chain lowers the PCE of OSCs in inverted configuration with $PC_{71}BM$ acceptor. Also in this case the fall of $J_{sc}$ is the ground of the poorer performances of mFIID and oFIID, due to the low hole mobility determined by the distortion from planarity between the phenyl pendant rings and the main conjugated chain induced by fluorine atom, especially in the orto position. On contrary, the introduction of fluorine atoms on thiophene based pendant chain in 4' position (PBQ-4F,[18] PM6,[19] PBDTT-SF-BDD,[20] PBDTT-SF-TT[20]) or in both 4' and 3' positions (PBDTT(FF)-ttTPD[21] seems not to show the drawbacks related to fluorination of pendant benzene rings. In DA copolymer PBQ-4F[18] both pendant thiophene moieties on the donor units and quinoxaline acceptor units bear fluorine substituents leading to devices ($PC_{71}BM$ as the acceptor and Ca/Al cathode) with high $V_{oc}$ (0.88 V), $J_{sc}$ (13.26 mA/cm$^2$), FF (70.10%) and excellent PCE (8.18%). These performances are further improved by using a cathode electrode consisting of aluminum and the polymeric electrolyte PFNBr (Fig. 3) as interlayer, reaching 9.04% PCE as consequence of an increased $J_{sc}$.

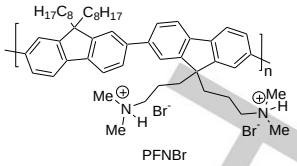


PFNBr

**Figure 3.** PFNBr polymer electrolyte

This effect is ascribed to a better arrangement of the PBQ-4F/$PC_{71}BM$ film with the PFNBr interlayer that promotes charge extraction and reduces charge recombination.

Copolymer PBDTT-SF-BDD [20] reaches 9.72% PCE in fullerene based OSCs characterized by high values of $V_{oc}$ (0.97 V) and $J_{sc}$ (14.70 mA/cm$^2$). This favourable balance between $V_{oc}$ and $J_{sc}$ may derive from a synergistic effect of the presence of fluorine atom and thioalkyl group on the pendant thiophene ring.

### 3.2. Oligomers and small molecules

Small molecules with π–extended conjugated system have been used as alternative donor materials to conjugated polymers in BHJ OSCs.[22] The most promising materials are molecular systems with donor-acceptor alternating units in structures that reproduce in small scale the same structural features of D-A polymers. Very high PCEs have been obtained in devices using such oligomers with well-defined structure, often coupled with non-fullerene oligomeric acceptors. The introduction of fluorine atoms on the donor or acceptor small molecules is a convenient structural modification for tuning their HOMO-LUMO levels to achieve the optimal separation between the HOMO of the donor and the LUMO of acceptor and increase $V_{oc}$, $J_{sc}$ and FF. In Chart 2, examples of the most performing oligomers and small molecules are reported along with a comparison with their non-fluorinated counterparts. Data on OSCs made with these materials are reported in Table 2.

Benzodithiophene and diketopyrrolopyrrole are donor and acceptor units, respectively, in the narrow band gap BDT-DPP oligomers[23] and fluoro or trifluoromethyl substituents are introduced on the phenyl rings at the end of the conjugated backbone. Both substituents decrease the HOMO level of oligomers without changing the bandgap and the photoabsorption properties. The strongest effect is demonstrated on BDT-DPP4 with two trifluoromethyl groups that exhibits the greatest $V_{oc}$ value. However, the PCEs of BDT-DPP2 and BDT-DPP4, bearing trifluoromethyl groups, are significatively lower than those bearing simple fluorine atoms as substituents (BDT-DPP1 and BDT-DPP3). Also in this case the reason lies in the lower values of $J_{sc}$. GIWAX data on the BHJ film of BDT-DPP oligomers and $PC_{71}BM$ acceptor clearly indicate a better packing along the π–π direction for BDT-DPP1 and BDT-DPP3, that is absent in BDT-DPP2 and BDT-DPP4, due to the steric effect of the bulkier trifluoromethyl groups versus simple fluorine atom. The enhanced charge transports through this ordered π-stacking allows higher $J_{sc}$ values for blends with BDT-DPP1 and BDT-DPP3.

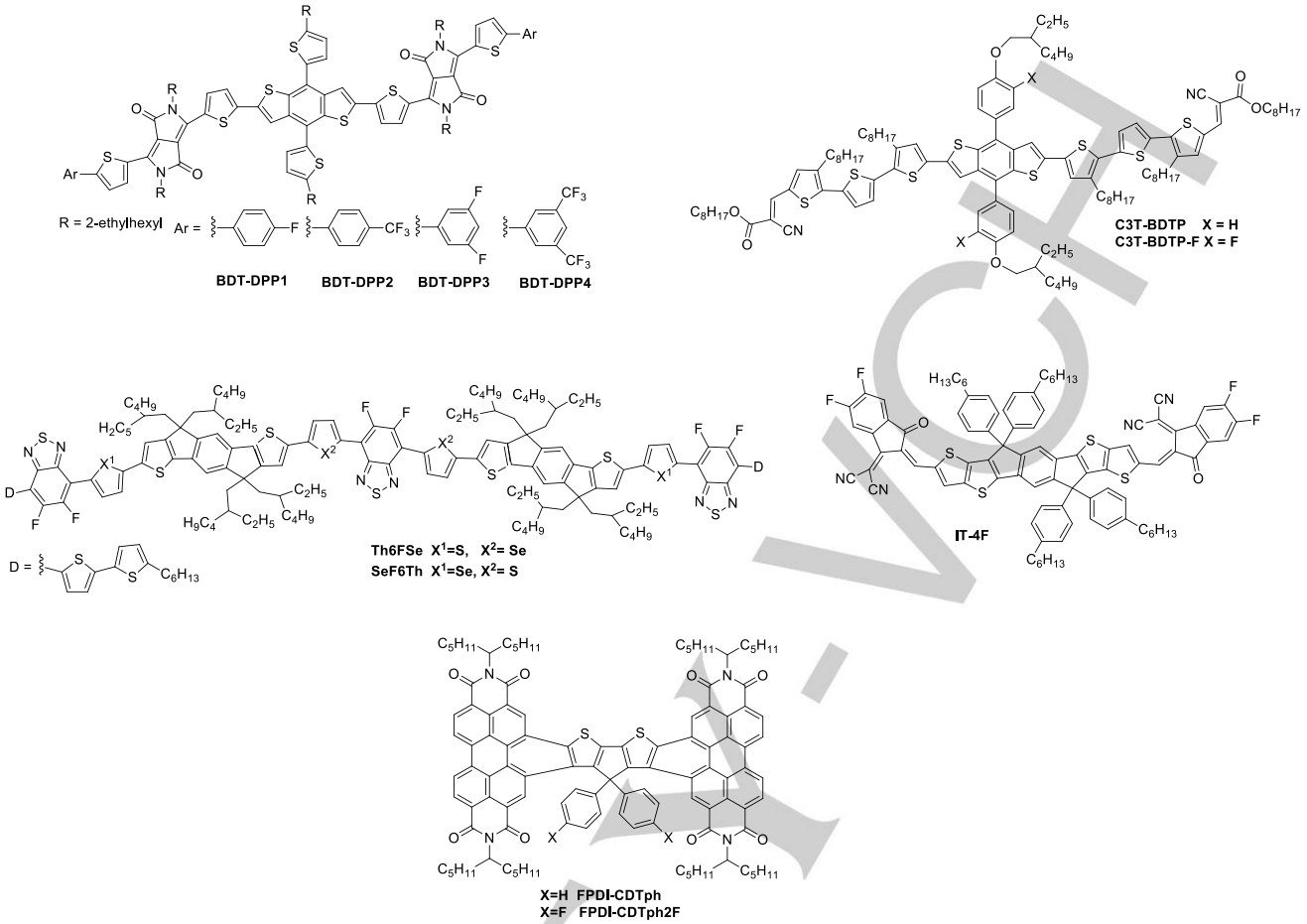


**Chart 2.** Conjugated oligomers and small molecules for OSCs

In C3T-BDTP and C3T-BDTP-F oligomers[4] the donor unit is represented by the cross-conjugated diphenyl benzodithiophene system and the acceptor unit by cyanoacrylate system. In C3T-BDTP-F, fluorine is placed on the donor unit in the meta position of the pendant benzene ring that, as found in the polymer PPh-m-F (Chart 1), should not disturb the planarity of the conjugated system. In devices with optimized architecture, the blend of C3T-BDTP-F, $PC_{71}BM$ and 1,8-diiodoctane as additive reaches a PCE of 5.30% against the value of 5.16% obtained with the non-fluorinated counterpart. As expected, fluorine atom increases the $V_{oc}$, but slightly decreases the $J_{sc}$. The result of an investigation on the morphological and optical properties of C3T-BDTP-F/$PC_{71}BM$ film, and on charge carrier mobilities indicates that the lower $J_{sc}$ can be attributed to absorption characteristics (red shift in EQE spectrum joined with a decrease of the extinction coefficient with respect of the non-fluorinated oligomer) and not to reduced hole mobility, that may derive from a unfavorable morphology of the film.

The highest PCE (9.3%) for a solution-processed BHJ-OSC with a D-A small molecule and $PC_{71}BM$ active layer has been recently obtained. The hexafluorinated Th6FSe and Se6FTh oligomers[25] have fluorinated benzothiadiazole acceptor units alternated with indacenotiophene donor moieties and are capped with 2,2'-bithiophene donor moieties. These conjugated structures (D-A-π-D-π-A-π-D-π-A-D type) present thiophene and selenophene rings as π bridges arranged in different sequence in the two oligomers. The inclusion of selenophene units is expected to extend the absorption range and increase the charge carrier mobility with a positive effect on the performances in OSCs. However, the beneficial effect depends on the position of selenophene π bridges in the conjugated backbone. Devices made with Se6FTh, bearing the selenophene bridges located next to terminal benzodithiazole units, and $PC_{71}BM$ shows higher PCE (5.40% against 4.17% of similar devices made with Th6FSe). The PCE reaches the highest value of 9.26% by an appropriate sequence of annealing processes (solvent vapour annealing followed by thermal one). This result highlights the role of the post-treatment of active films in enhancing their performances by achieving more ordered and crystalline morphology. The response of Th6FSe and Se6FTh to the annealing treatment is however different: the AFM and high resolution TEM images of the film obtained from Se6FTh show a better bicontinuous morphology of disperse fibrous structures of 15-20 nm after the sequence of annealing processes, whereas smaller domain sizes occur in the case of films made with Th6FSe. Moreover, GIXD X-ray diffraction technique clearly show a compact stacking for Se6FTh with strong intermolecular interactions. Therefore, the position of selenophene rings play a critical role in determining the optimal morphology of these oligomers in the film for more efficient OSCs.

**Table 2.** Characteristic parameters for OSCs made with oligomers/small molecules in Chart 2

| Oligomer/small molecule | PCE (%) | $V_{oc}$(V) | $J_{sc}$(mA cm$^{-2}$) | FF (%) |
|---|---|---|---|---|

| | | | | |
|---|---|---|---|---|
| BDT-DPP1 | 4.0 | 0.76 | 10.1 | 52.0 |
| BDT-DPP2 | 2.8 | 0.83 | 6.1 | 54.0 |
| BDT-DPP3 | 4.2 | 0.85 | 8.3 | 60.0 |
| BDT-DPP4 | 1.1 | 0.94 | 2.5 | 45.0 |
| C3T-BDTP | 5.27 | 0.91 | 9.7 | 60.1 |
| C3T-BDTP-F | 5.42 | 0.97 | 8.8 | 63.6 |
| Th6FSe | 4.17 | 0.86 | 10.10 | 49.0 |
| Th6FSe [a] | 4.83 | 0.83 | 12.34 | 67.0 |
| Th6FSe [b] | 4.27 | 0.87 | 9.72 | 50.0 |
| Th6FSe [c] | 6.84 | 0.87 | 11.78 | 67.0 |
| Th6FSe [d] | 6.44 | 0.85 | 11.23 | 67.0 |
| Se6FTh | 5.40 | 0.90 | 11.18 | 54.0 |
| Se6FTh [a] | 7.87 | 0.87 | 12.75 | 71.0 |
| Se6FTh [b] | 5.55 | 0.90 | 11.54 | 53.0 |
| Se6FTh [c] | 8.13 | 0.86 | 13.56 | 71.0 |
| Se6FTh [d] | 8.95 | 0.87 | 14.30 | 72.0 |

[a] With Solvent Vapour Annealing (SVA); [b] with Thermal Annealing (TA); [c] with TA + SVA; [d] with SVA + TA

More recently small molecules have been also proposed as electron acceptors in BHJ OSCs, in substitution of fullerene derivatives.[26] These non-fullerene acceptors (NFA) offer some advantages over fullerene, such as ease of synthesis, better solubility and processability from organic solvents, greater optical absorptivity that contribute to photocurrent generation by n-type excitation and hole transfer to electron donor material. On the other hand, NFAs are weaker electron acceptors than fullerenes and, owing to a reduced HOMO-LUMO offset ($\Delta_{LUMO}$), they work well with wide-gap donor materials to afford acceptable values of $V_{oc}$. Considering that low band-gap donor materials are the most useful materials in OSCs, owing to their greater absorption in the visible range, suitable NFAs materials with a wider $\Delta_{LUMO}$ are desirable. The introduction of fluorine atoms may enlarge this value by lowering the HOMO level. Two example of fluorinated NFA are discussed below.

ITIC (Fig. 2) has the fluorinated counterpart IT-4F[27] that allows to reach a very high PCE value (13.10%) in BHJ devices made using the fluorinated PBDTT-SF-BDD polymer (Chart 1) with respect to the same device made with the non fluorinated counterparts (PCE 11.05%) or with the fluorinated acceptor polymer and conventional $PC_{71}BM$ (PCE 8.89%). This striking performance is due to the favorable alignment of molecular energy levels down-shifted by the presence of fluorine atoms on both the active materials, but also by a broader absorption range and enhanced absorption coefficient of the active layer that improve remarkably the $J_{sc}$ value.

Perylenedimide derivatives are characterized by intense light absorption, high electron mobilities and good thermal stability that make these molecules suitable candidates as acceptor materials in non-fullerene OSCs. FPDI-CDTph and FPDI-CDTph2F[28] have been proven as efficient acceptors in BHJ active layers with the fluorinated polymer PTB7-Th. Better performances have been obtained for devices with FPDI-CDTph2F (PCE 6.03% versus 4.10% of the non fluorinated acceptor). The higher value of efficiency is mainly due to an increased $J_{sc}$ in the device with the fluorinated acceptor. Fluorine atoms influence the BHJ morphology leading to an optimal separation and interconnection of domains that originate an efficient exciton dissociation and balanced charge transport.

### 3.3. Metal complexes

Among organometallic complexes, fluorinated copper phthalocyanines have been reported as efficient electron transporting materials for photovoltaic applications.[29] Deposition of nanowires of copper hexadecafluorophthalocyanine ($F_{16}CuPc$ in Fig. 4) between the indium tin oxide anode and the n-type semiconducting ZnO layer was found to enhance (*i*) the interfacial electron transport in inverted solar cells, (*ii*) the short circuit current densities ($J_{sc}$) and (*iii*) the power conversion efficiencies (PCE) versus the cells made only with ZnO layers (PCE 3.6% *vs* 3.0% and 8.6% *vs* 8.1% for P3HT:$PC_{61}BM$ and PTB7:$PC_{71}BM$ cells, respectively).[29a] Such improvement was attributed to the stable n-type semiconducting properties of $F_{16}CuPc$, the face-on alignment of the π-stacked nanowires along the device current flow direction and the enhanced surface area of $F_{16}CuPc$ nanowires embedded in the ZnO film.

Fluorinated boron phthalocyanines have also deserved scientific interest for photovoltaics. In general, metal phthalocyanines act as electron donor materials but fluorination increases their ionization potential with minimal changes to the optical bandgap and converts them into electron acceptor molecules.[30] Verreet *et al.* synthesized fluorinated fused boron subphthalocyanine dimers (FSubPcDimer in Figure 4) in both *syn* and *anti* configurations and demonstrated that they are efficient acceptor materials with complementary absorption to the non-fluorinated boron subphtalocyanine (SubPc).[31] A solar cell based on the SubPc/FSubPcDimer photoactive D/A pair was obtained, with high open circuit voltage ($V_{oc}$=960 mV), moderate short-circuit current density ($J_{sc}$=5.1 mA/cm$^2$) but low field factor (*FF*=24%), due to poor charge extraction. In a solar cell with PCE of 4%, the *FF* was improved to 54% by insertion of a $C_{60}$ electron transporting layer that promoted the charge extraction from the FSubPcDimer.

A series of fluorinated azadipyrromethene zinc(II) complexes was also reported as promising electron acceptors in bulk

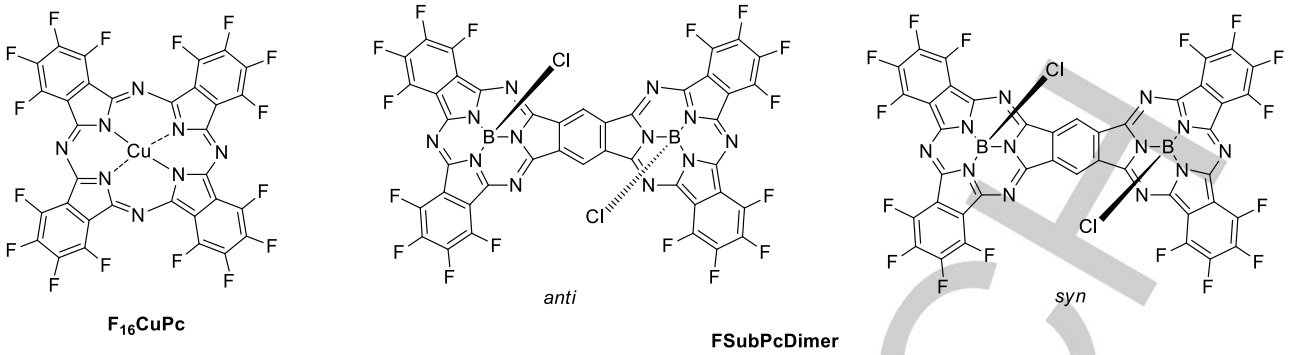


**Figure 4.** Metal complexes for OSCs

heterojunction OPVs with inverted configuration, using P3HT as the electron donor. Fluorination was found to have little effect on the optical properties of zinc(II) complexes but to be beneficial for their performances in devices, leading to an increase of PCE values, due to an increase of $J_{sc}$, versus devices made with the non-fluorinated analogue.[32]

## 4. Organic fluorinated materials for thin film transistors

### 4.1. Conjugated polymers

OFETs have been introduced in late 1980s[33] as organic alternative to the silicon-based devices. Only in the last two decades, however, they have reached performance levels comparable to their inorganic counterparts, by the introduction of π-conjugated polymers as semiconductor materials. OFETs add to the transistor technology features of low-cost, large-area, mechanically flexible and disposable electronics.[34]
Most conjugated polymers exhibit unipolar hole-transport behaviour. Logic circuits require materials with ambipolar properties able to effectively and selectively transport either hole and electron charge carriers.[35] The D-A conjugated polymers, successfully used for OSCs, have been employed to this purpose and n-type or ambipolar behaviour is depending on the acceptor units in the conjugated backbone. Fluorination of D−A copolymers backbone is an effective strategy to enhance the electron transport properties in OFETs; the main effect of fluorine atom, as discussed for OPV polymers, is to lower both the HOMO and LUMO energy levels. Changes in crystallinity, internal polarization, and morphology of the active layer can also be originated by the presence of fluorine atoms on the conjugated backbone. In Chart 3, some examples of the most performing D-A (or D-π-A) polymers are reported along with a comparison with their non-fluorinated counterparts.
PDPP-FBT and PDPP-2FBT polymers[36] contain two most popular acceptor units, benzothiadiazole and diketopyrrolopyrrole, and one (PDPP-FBT) or two (PDPP-2FBT) fluorine atoms are present on the benzothiadiazole unit. Both polymers exhibit ambipolar behaviour (electron mobility up to 0.42 $cm^2 V^{-1} s^{-1}$ and hole mobility 0.15 $cm^2 V^{-1} s^{-1}$) which likely result from high electron affinity of π-system and strong intermolecular interaction induced by fluorine atom. In fact, 2D-GIXD analysis reveals long range lamellar packing of the polymer chains and a dense π–π stacking after a thermal annealing process. The edge-on orientation of this molecular packing is very effective for the charge transport between the source and drain electrodes.
Simple D-A P1 and P2 polymers [37] bear diketopyrrolopyrrole as acceptor units and bithiophene as donor units. P1 shows an ambipolar behaviour with hole mobility slightly higher than electron mobility (0.22 vs 0.19 $cm^2V^{-1} s^{-1}$). The introduction of fluorine atom in the P2 increases significantly hole and electron mobilities (0.80 and 0.51 $cm^2 V^{-1} s^{-1}$) with acceptable $I_{on}/I_{off}$ ratio ($10^3$ for p-channel and $10^2$ for n-channel). The position of the fluorine atom on the thiophene moiety was chosen on the basis of density functional theory conformation analyses. Theoretical calculations reveal a marked distortion from planarity when fluorine atom is pointing towards the diketopyrrolopyrrole unit (3-position of thiophene ring). On the contrary, planarity is not significantly disturbed when the fluorine atom is placed on the other side of the thiophene ring (4-position).
In P3-P5 polymers, [38] a ladder planar structure is induced by alternation of indacenothienothiophene donor and fluorinated benzothiadiazole acceptor units. The charge transport properties are modulated inserting in the conjugated chain diketopyrrolopyrrole as further acceptor unit (P3) or benzodithiophene donor unit cross-conjugated with thiophene (P4) or selenophene (P5) units. P3 is an effective ambipolar semiconductor with a balanced charge carrier mobilities for holes and electrons (μ =0.0068 and 0.0130 $cm^2V^{-1} s^{-1}$). On the other hand, P4 and P5 are hole transporters (μ = 0.0227 and 0.0300 $cm^2V^{-1} s^{-1}$, respectively). This behavior is explained on the basis of the relative HOMO and LUMO energies and of the low band-gap of P3, due to the presence of the additional acceptor unit, with respect to the levels of P4 and P5. This structural feature facilitates the injection of either holes and electrons using Au for source and drain electrodes, owing to the low injection barrier. The use of PMMA as material for the gate dielectric layer also plays a significant role, owing to the presence of few electron-trapping groups in this polymer.
The benzodifurandione based acceptor has been proven to be an effective electron deficient core. In polyphenylenevinylene (PPV) derivatives FBDPPV-1 and FBDPPV-2[39] including this unit the presence of fluorine atoms locks the conformation of the conjugated chain through the H⋯F interactions. Moreover, both polymers have the lowest value (-4.26 and -4.30 eV, respectively) of the LUMO level reported in the literature. These two features, greatly enhance the electron mobilities: μ =1.70 $cm^2V^{-1} s^{-1}$ has been reached with FBDPPV-2 in an OFET operating in ambient conditions. On the other hand, a significantly lower value (μ=0.81 $cm^2V^{-1} s^{-1}$) was obtained in the device with FBDPPV-2. These results indicate a strong influence of the conformation of the polymer backbone on the charge transport ability. Both polymers have comparable electrochemical and physical properties, and the resulting thin films show the same morphology and packing of the polymer chain. On the other hand, computational analysis shows that stable interactions between the H atom of the vinylene units and the fluorine atoms are present, but these interactions depend on their relative positions. Different conformations of the conjugated chains are highlighted by theoretical calculations for FBDPPV-1 and FBDPPV-2, and their presence is confirmed by

single crystal X-ray analysis. This study evidences that the effects of fluorination on the charge carrier mobility acts not only on to the energy levels of the conjugate system but also on the conformational differences derived from the position occupied by the fluorine atoms on the conjugated chain.

The importance of the conformational arrangement induced by fluorine atoms has been also highlighted in polythiophenes or polythiophene-like materials. Three 3-fluoro-4-alkylpolythiophenes (F-P3HT, F-P3OT, F-P3HET)[40] differing in the alkyl chain length and branching have been compared with the corresponding non-fluorinated counterparts, and a considerable increase of the ionization potential was evidenced for the fluorine substituted polymers. Moreover, fluorinated and non-fluorinated polymers show the same optical band gaps, indicating that the presence of fluorine atoms lowers both HOMO and LUMO levels of nearly the same amount. All these polymers behave as p-type semiconductors and an increase of the hole mobilities is noticed when moving from the non-fluorinated to the fluorinated materials. The highest mobility measured in OFETs is $\mu$=0.7 $cm^2V^{-1}$ $s^{-1}$ for F-P3OT with a linear octyl chain, about five time higher than that of P3OT ($\mu$=0.14 $cm^2V^{-1}$ $s^{-1}$). Such high value of mobility is due not only to the electronic effects of fluorine atoms but also to the rigid and planar conjugated chain with all thiophene rings coplanar to one another and sulfur atoms facing the fluorine atoms, in a transoid conformation with respect to the sulfur atoms of adiacent thiophene rings. The electrostatic interactions between these atoms appear to be the driving force for such spatial arrangement leading to a strong aggregation and packing in the solid state in an edge-on orientation of the chains that contributes significantly to the charge carrier mobility. However, this aggregation does not correspond to an increase of crystallinity in the thin-film with respect to P3OT, as evidenced by GIWAXS analysis. The stiffness of F-P3OT due to the presence of fluorine atoms and the high rotational barrier (ca 10 KJ/mol) prevents the reorganization of the chain segments in less stable cisoid conformation of adiacent thiophene rings and crystallization in the solid state.

The S-F interactions are also effective in P3HT-50F, P3HT-33F, P3HT-25F,[41] regioregular polymers with different content of fluorine atoms. The higher values of hole mobility are measured for P3HT-33F ($\mu$=2.72 $cm^2V^{-1}$ $s^{-1}$, after annealing of the film at 150°C). The S-F interactions, as discussed above, stabilize a highly planar arrangement with thiophene rings in transoid conformation in the chain regions where the fluorinated rings are present. The best results of P3HT-33F with respect to polymers with higher or lower degree of fluorination may be explained as the optimum trade-off between the increase of planarization and the decrease of crystallinity, as discussed above.

Finally, the about four time higher hole mobility of thiophene-thienothiophene FBTTT[42] versus the non-fluorinated BTTT (from $\mu$=0.058 to $\mu$=0.23 $cm^2V^{-1}s^{-1}$) is explained on the basis of the more planar conformation of the conjugated chain, due to S-F interaction. The resulting enhanced aggregation and edge-on order are the main reasons for the higher mobility in the FBTTT based OFET.

Fluorine atoms have been introduced not only on the conjugated chain of semiconducting polymers but also in the pendant alkyl chains, that confer solubility for solution processability. A significant increase of hole mobility is demonstrated in PDPP-BT[43] ($\mu$= 6.01x$10^{-2}$ $cm^2V^{-1}s^{-1}$) when the alkyl chain on the diketopyrrolopyrrole unit is replaced by a semi-fluorinated chain (PFDPP-BT; $\mu$= 0.24 $cm^2V^{-1}$ $s^{-1}$). Obviously, the fluorine atoms in these positions have only minimal influence on the HOMO/LUMO levels and on the band-gap. On the other hand, these partially fluorinated chains significantly affect the morphology and microstructure of thin films. AFM and XRD analysis established a higher crystallinity degree in thin film derived from PFDPP-BT with respect to the non-fluorinated counterpart. The enhancement of charger carrier mobility is an effect of improved packing of the polymer chain in the solid-state and of the film morphology induced by the presence of fluorine atoms rather than the electronic effects on HOMO/LUMO energy levels.

Also the materials used in dielectric layers of the transistor configuration can play a synergistic effect with the presence of fluorine atoms in the polymer structure. In PDFDTV,[44] an impressive increase of hole mobility from $\mu$=0.24 to $\mu$=9.05 $cm^2V^{-1}$ $s^{-1}$ is obtained by using high-*k* ferroelectric fluorinated polymers P(VDF-TrFE-CTFE), poly(vinylidenefluoride-trifluoroethylene-clorotrifluoroethylene), as gate dielectric, instead of PMMA. This significant increase is mainly due to the improved positive charge carrier accumulation at the interface gate-semiconducting layer, which is characteristic of this gate insulator.

### 4.2. Oligomers and small molecules

Small molecules and oligomers with a defined structure show a greater tendency, compared to polymeric materials, to form ordered crystalline domains that enhance the charge carrier mobility. The application of molecular organic semiconductors in OFETs has been recently reviewed.[3b] In our survey, just recent examples of fluorinated oligomers and small molecules, reported in chart 4, has discussed.

Charge transfer complexes between benzothienothiophene (BTBT)[45] with tetracyanoquinodimethane ($F_n$TCNQ n= 0, 2, 4) and benzoselenobenzoselenophene (BSBS) with $F_2$TCNQ show n-type charge transport and the S4 complex shows the higher value of electron mobility ($\mu$=0.054 in vacuum and $\mu$=0.043 $cm^2V^{-1}$ $s^{-1}$ in air) in a single crystal OFET, which persists almost unchanged after 8 months of preservation under vacuum. The other complexes (S0, S2, Se2) show electron mobilities about one order of magnitude lower. However, all complexes show poorer performances in thin-film OFETs. The higher electron mobility in single crystal with respect to thin film appears to be strictly related to the perpendicular arrangement of molecular plane on the substrate. This solid-state arrangement (side-on) is considered very advantageous for transistor performances and XRD investigation shows that all complexes exhibit such molecular packing with molecular planes slightly tilted from the normal to the substrate. For complex S4 the monoclinic crystal lattice grants a near perpendicular arrangement that maximizes the charge mobility.

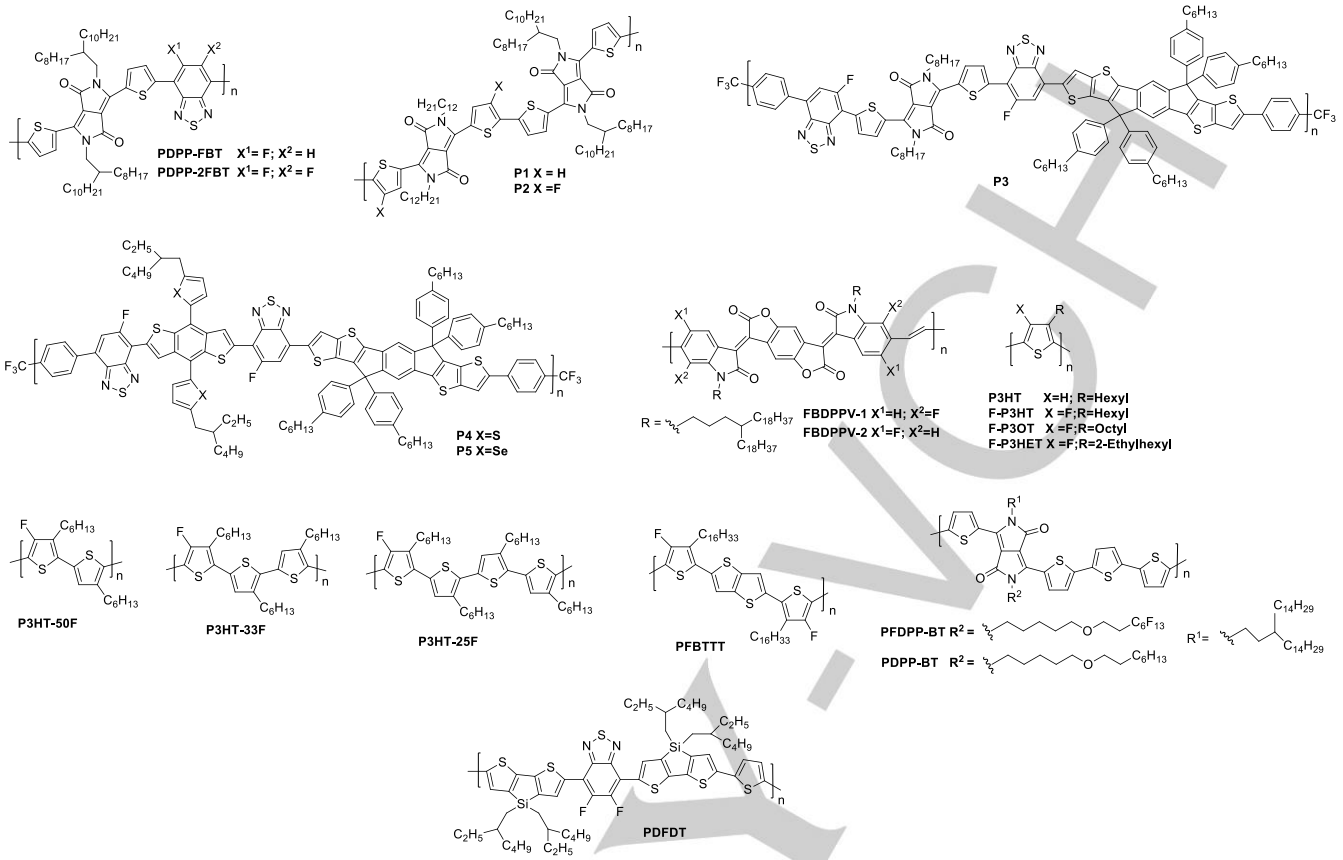


**Chart 3.** Conjugated polymers for OFETs

The compact and electron deficient core of naphtalenediimides (NDI) makes them potential n-type semiconductors in OFETs. The high electron mobility of simple unsubstituted NDI (6.2 $cm^2V^{-1}$ $s^{-1}$) is rapidly degraded in air.[46] Air-stable OFETs can be obtained by introduction of electron-withdrawing substituents which lower the LUMO level and improve the air stability. Naphtalenedimides 2FNDI-1a-d, 4FNDI-2a-b, 2FNDI-3, and 2FNDI-4[47] differ in the presence of two or four fluorine atoms, alkyl chain on the imide nitrogen atoms, or the presence of additional fused quinoxaline system, also bearing two electron-withdrawing groups. In fact, all these molecules are characterized by a low-laying LUMO level with the lowest values of -4.27 and -4.54 eV for 2FNDI-3 and 2FNDI-4, respectively, that make these compounds ultra-strong electron acceptors. The highest values of electron mobilities were measured for 4FNDI-2a ($\mu$=0.02 $cm^2V^{-1}$ $s^{-1}$) and 2FNDI-1c ($\mu$=0.1 $cm^2V^{-1}$ $s^{-1}$) in OFETs with active layer obtained by thermal evaporation of the semiconducting materials. These rather poor performances, if compared to other similar NDI derivatives bearing two chlorine atoms (N,N'-bis(perfluorobutyl)-2,6-dichloroNDI), are ascribed to the crystalline structures of these derivatives. The herringbone molecular packing of fluorine substituted NDI shows larger $\pi$–$\pi$ interaction distances with respect to the chlorine substituted NDI, with a lower packing density, despite the smaller dimension of the fluorine atoms. Moreover, the lower slipping angles of the packing of 4FNDI-2a and 2FNDI-1c (48° and 46°) with respect the N,N'-bis(perfluorobutyl)-2,6-dichloro NDI (62°) may also reduce the contact between the electrodes and the semiconductor molecules leading to poorer OFET performances of the fluorinated NDI.

Cyclopentadithiophene (CPD)[48] derivatives with the corresponding fluorinated derivatives have also been reported. Beside the introduction of fluorine atoms, electron withdrawing groups (carbonyl, dicyanomethylene) are also present on the bridgehead position of the CPD. The evaluation of the HOMO/LUMO levels of these compounds shows that the effect of electron withdrawing groups on this position is to lower the LUMO levels, and the dicyanomethylene has the greater effect. By replacing the phenyl rings on the $\alpha$ position of the CPD nucleus with pentafluoro substituted phenyl rings, a decrease of the HOMO level is achieved together with a slight increase of the LUMO level. This observation leads to the conclusion that the presence of a strong electron withdrawing group on the bridgehead position dampens somewhat the effect of the substituents in the $\alpha$ positions. The charge transport characteristics are switched from p-type conduction for the non-fluorinated materials to n-type by fluorination, although the mobilities values are rather low ($\mu$=$10^{-4}$-$10^{-5}$ $cm^2V^{-1}$ $s^{-1}$ for both hole and electron transport). The authors could not establish the reasons of this behaviour that cannot be explained only on the basis of frontier orbital energy levels.

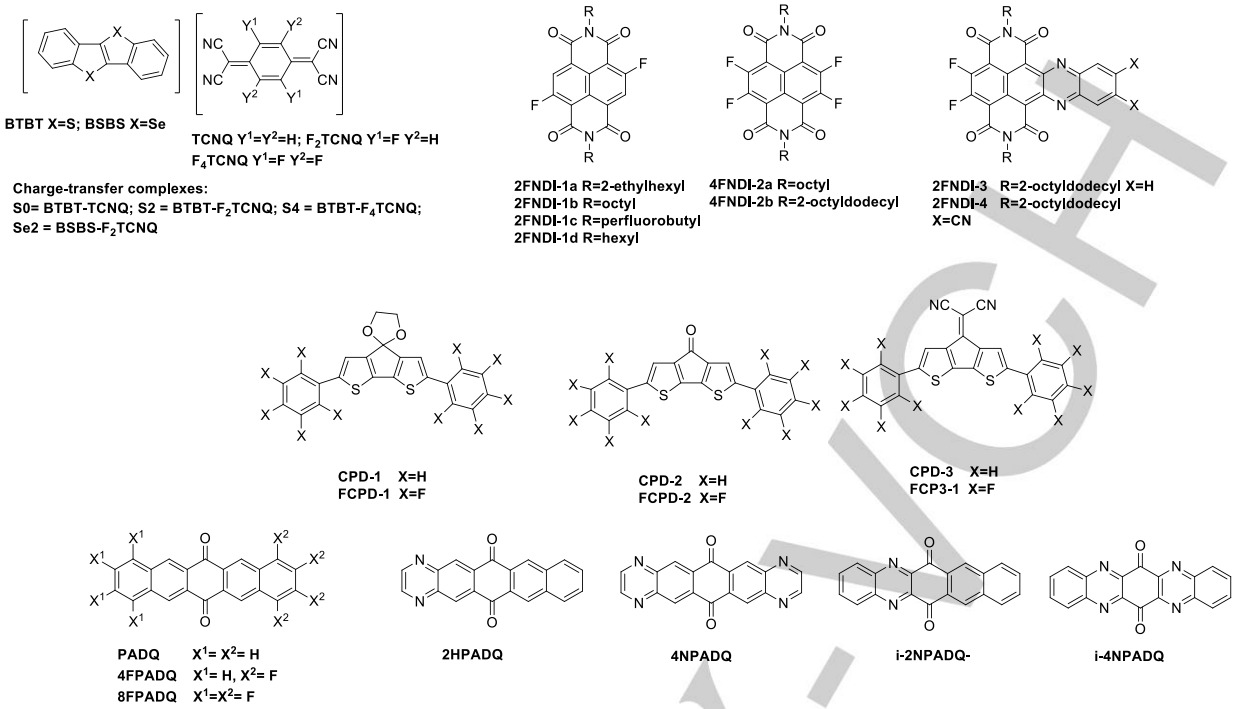


**Chart 4.** Conjugated small molecules for OFETs

Pentacene derivatives are small-molecules that have been extensively used as semiconductors in OFETs and are considered as benchmark for molecular semiconducting materials. Pentacenequinones (PAQ) are similar rigid and planar molecules less commonly used as molecular semiconductors in organic electronics. Some pentacenequinone derivatives[49] are reported in Chart 4. They are functionalized by introduction of electron-withdrawing substituents as fluorine atoms or including N-heteroaromatic nuclei in the core of the polyaromatic structure, with the aim of lowering the LUMO level and switching the charge carrier transport properties from p-type to n-type. The highest electron mobilities obtained in thin film OFETs are provided by the fluorinated derivative 8FPADQ and the heterocyclic derivative i-4NPADQ ($\mu$=0.18 and $\mu$= 0.12 $cm^2V^{-1}$ $s^{-1}$, respectively). XRD analysis of pentacenequinones shown that 8FPADQ and i-4NPADQ form polycrystalline films with polymorphs different from the bulk crystals. The other derivatives originate substantially amorphous films. The crystalline nature of 8FPADQ film is the rationale of its higher values of electron mobilities that cannot be related to electronic structures or to molecular packing.

### 4.3. Metal complexes

Among organometallic complexes, fluorinated metal phthalocyanines have been investigated as semiconductors for organic field effect transistors.[50]High-quality and large-size organic single crystals of copper, cobalt and zinc hexadecafluorophthalocyanines ($F_{16}$CuPc Fig. 4, $F_{16}$CoPc and $F_{16}$ZnPc) were used by Jiang *et al.* to fabricate *n*-channel single crystal organic field effect transistors.[51] Fluorination confers n-type semiconducting properties to the corresponding p-type metal phthalocyanines but it significantly lowers their electron mobility in thin films or in single crystals. However, the nature of the central metal ion (Me) was found to influence the intermolecular spacing distance and, as a consequence, the intermolecular interactions and charge mobilities in single $F_{16}$MePc crystals. The best charge mobility ($\mu$~1.1 $cm^2V^{-1}s^{-1}$) was recorded for $F_{16}$ZnPc and the high value can be explained by high electron transfer integrals and weak electron-phonon coupling strength found for this complex by theoretical calculations.

Fluorinated copper phthalocyanines ($F_x$CuPc, x=4, 8, 12, 16) were also used as semiconductors for single-component organic thin-film transistors (OFETs).[52] In fact, the $F_x$CuPc semiconducting behavior was found to be tunable form p-type to ambipolar and finally n-type by properly selecting the degree of fluorination.[52] In particular, the OFET with $F_{12}$CuPc showed an ambipolar performance with carrier mobilities in air of $\mu$=0.005 $cm^2$ $V^{-1}s^{-1}$ for holes and $\mu$=0.006 $cm^2$ $V^{-1}s^{-1}$ for electrons. Increasing the number of electron withdrawing fluorine atoms in $F_x$CuPc, a decrease of the HOMO and the LUMO energy levels was observed, favoring electron injection and ambient stability of complexes. Moreover, a high number of fluorine atoms promote molecular $\pi$–$\pi$ stacking and lead to more continuous $F_x$CuPc film morphology, thus enhancing their carrier mobility in devices.

## 5. Organic fluorinated materials for OLEDS

### 5.1. Conjugated polymers

Compared to fluorinated materials for photovoltaics, a more limited number of novel fluorinated organic polymers has been developed and used in the last decade for OLEDs.

A series of poly(arylenevinylene)s with fluorinated vinylene units was synthesized by our group,[53] and combined theoretical and spectroscopic studies were carried out on the MEH-PPVF [poly(2-methoxy-5-(2'-ethylhexyloxy)-1,4-phenylene-difluoro-vinylene] polymer shown in Figure 5. Fluorination of vinylene

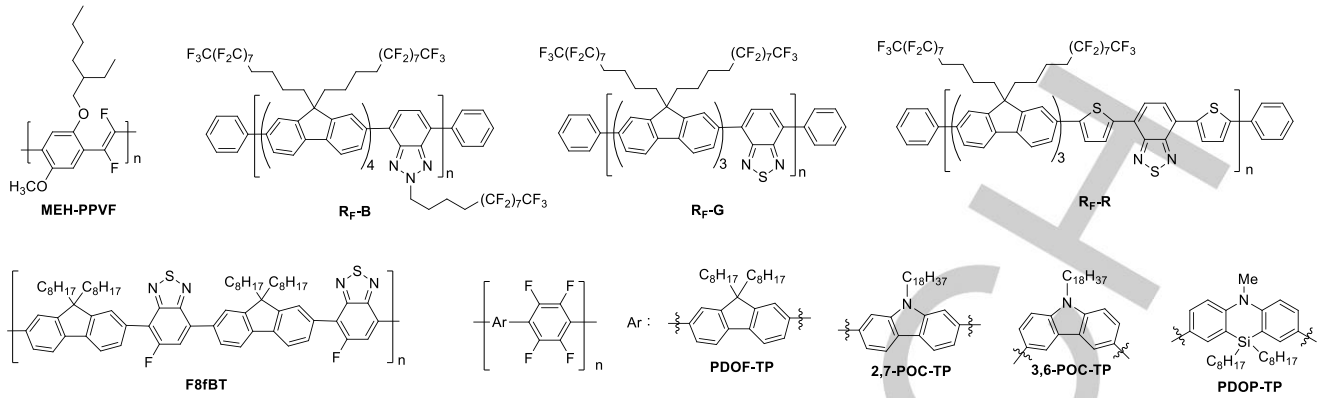


**Figure 5.**Conjugated polymers for OLEDs

units was found to significantly blue shift both light absorption and emission and to increase the energy gap of MEH-PPVF with respect to the non-fluorinated MEH-PPV polymer.[54]

Such behavior is not caused, as it could be expected in principle, by the electron withdrawing effect of fluorine atoms, but by the steric repulsion between the fluorine atoms on the vinylene units and the oxygen atoms on the aromatic rings. This repulsion causes a strong distortion of the MEH-PPVF conjugated backbone and reduces its effective conjugation length with respect to that of the non-fluorinated reference polymer.[55] The strong twist in the MEH-PPVF backbone also persists in the excited state, thus broadening the polymer emission spectrum, enhancing non-radiative deactivation and reducing the radiative rate and fluorescence quantum yield of MEH-PPVF versus MEH-PPV. Homogeneous blue-greenish electroluminescence was also observed for a MEH-PPVF based light emitting device with a simple configuration, with an EL maximum at 2.46 eV (corresponding to 504 nm) that is blue shifted versus that of MEH-PPV (1.98 eV, 625 nm).[56]

Fong *et al.* developed a series of blue, red and green light emitting copolymers ($R_F$-B, $R_F$-R, $R_F$-G in Figure 5) with semi-perfluoroalkyl side chains that, due to the presence of fluorine atoms, are soluble in fluorinated solvents, such as bis(trifluoromethyl)benzene (BTMB) and hydrofluoroethers (HFEs), but insoluble in common organic solvents, including xylene, toluene and chlorobenzenes.[57] These polymers have advantageous thin film properties, since the film surface is both hydrophobic, thus repelling moisture, and lipophobic, being resistant to direct contact with photoresist solutions and aqueous base photolithographic developers. This allowed multi-layer solution processing of polymers in OLEDs with stacked configuration, as well as patterning of polymers in RGB arrays via standard photolithography and dry etching in oxygen plasma.

A highly regioregular polymer (F8fBT in Figure 5) based on alternated 9,9'-dioctylfluorene and 5-fluorobenzothiadiazole monomeric units was synthesized and the effects of the regular fluorine substitution on molecular geometry and optoelectronic properties were investigated.[58] Fluorine atoms slightly increased the dihedral angle between fluorene and BT units, enhanced the ionization potential, and led to a slight hypsochromic shift of absorption and photoluminescence versus those of the non-fluorinated polymer (F8BT). F8fBT exhibited about 1 order of magnitude higher electron mobility versus F8BT, likely because the higher electron affinity of the fluorine substituent versus the hydrogen atom, contributes to lower the F8fBT LUMO level, thus favoring electron injection.

Fluorinated polymers were also proposed as efficient host materials for phosphorescent OLEDs. Poly(*N*-vinyl-2,7-difluoro-carbazole) (2,7-F-PVK) was, in fact, reported as a wide energy gap host polymer leading to exciton energy confinement on the blue FIrpic dopant emitter [FIrpic: iridium(III) bis[2-(4,6-difluorophenyl)pyridinato-N,C2]picolinate].[59] Solution-processed blue PHOLEDs based on FIrpic doped 2,7-F-PVK layer reached performances higher than those of a reference device made with the non-fluorinated PVK host, as an effect of the energy-gap-widening of fluorination in the host material. A series of fluorinated copolymers (PDOF-TP, 2,7-POC-TP, 3,6-POC-TP and PDOP-TP in Figure 5) was also synthesized via direct arylation of 1,2,4,5-tetrafluorobenzene with various dibromoarylenes and used as efficient hole-blocking layers in OLEDs, owing to their low HOMO levels related to the strong electron-withdrawing nature of fluorine substituents.[60]

### 5.2. Conjugated oligomers and small molecules

With regard to small molecules for OLEDs, a variety of fluorine substituted organic compounds with different chemical structures has been reported, including fluorinated triphenylamines,[61] perylene bisimides,[62] fullerenes,[63] oligophenylenes,[64] oligoarylenevinylenes,[65] anthraquinone based molecules.[66] Fluorination was found to influence electron transport properties, affecting molecular orientation and intermolecular interactions such as π-π stacking or hydrogen bonding. Kido *et al.* recently reported a series of fluorinated phenylpyridine-based materials and investigated the effect of fluorination on their molecular orientation and performances as electron transporters in phosphorescent blue OLEDs.[67] In particular, the best results were found for the monofluorinated B3PyMFB derivative (Figure 6), showing relatively large orientation order parameters and an electron mobility ($10^{-3}cm^2V^{-1}s^{-1}$) 10 times higher than that of the non-fluorinated B3PyPB counterpart, due to concerted intermolecular interactions based on π–π stacking, CH···N and CH···F hydrogen bonding.[67] Increasing the number of fluorine atoms, the orientation order parameter surprisingly decreases due to lower interactions between fluorine and nitrogen lone pairs. New bipolar fluorinated 3,3'-dimethyl-9,9'-bianthracene derivatives (MBAnFs in Figure 6) have been recently synthesized by Si *et al.* and applied as deep-blue emitters and host materials in OLEDs. In particular, both non-doped and doped multilayer light emitting devices based on the MBAn-(4)-F emitter have reached high external quantum efficiencies (EQE>6%) and CIE coordinates that well match the pure deep blue electroluminescence required by the European Broadcasting Union standard (0.15, 0.06).[68] Moreover, when used as the host layer for the blue DSA-ph dopant [*p*-bis(*p*-N,N-diphenyl-aminostyryl)-benzene], MBAn-(4)-F led to a device with

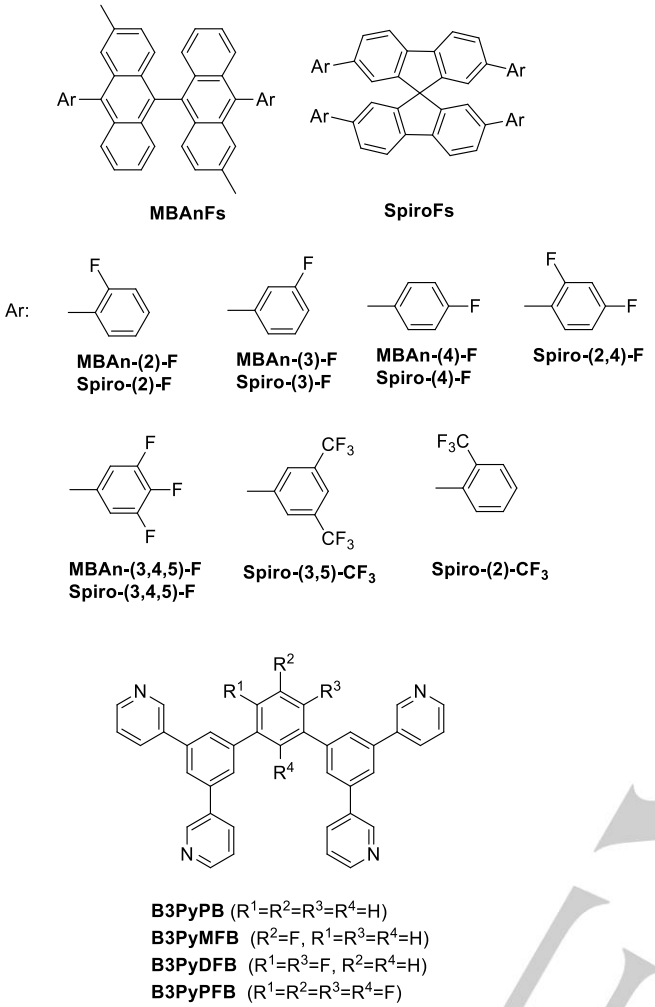


**Figure 6.** Conjugated small molecules for OLEDs

significantly high current efficiency of 23.01 cd $A^{-1}$ and a EQE of 11.52% with negligible efficiency roll-off. Such performances have been related to a good control of bipolar properties of MABn-(4)-F, leading to a good charge balance in the emitting layer.

Fluorinated 9,9'-spirobifluorenes (SpiroFs in Figure 6) were used as blue emitting host materials with high carrier mobility for fabrication of blue OLEDs. In particular, the device based on the Spiro-(3)-F host (Figure 6) showed low turn-on voltage of 3.4 V, and very high luminance of over 10000 cd $m^{-2}$, high current efficiency of 6.66 cd $A^{-1}$ and external quantum efficiency of 4.92%.[69]

### 5.3. Metal complexes

Among organometallic complexes, fluorine substituted iridium emitters still represent, in the last decade, the most investigated fluorinated phosphors for light emitting devices.

Liu *et al.* observed that, for the homoleptic $Ir(BFPPya)_3$ and $Ir(BDFPPya)_3$ complexes (Figure 7) with fluoro- and difluorophenylpyridazine ligands, both photoluminescence quantum yields and phosphorescence lifetimes increase with the number of fluorine atoms, likely because molecular vibration and, hence, non-radiative decay processes are reduced replacing C-H with C-F bonds.[70] However, increasing the number of fluorine atoms, the thermal stability and conductivity of complexes in devices decrease, likely due to the reduction of the Dexter energy transfer from the TPBI [2,2',2"-(1,3,5-benzenetriyl)tris(1-phenyl-1*H*-benzimidazole)] host to the more fluorinated emitter.

Heteroleptic fluorinated complexes bearing two arylpyridine-type and one different ancillary ligand bound to iridium, have been most frequently used for OLED applications with respect to the homoleptic counterparts, mainly because of their easier synthetic procedures. Our group reported a series of heteroleptic iridium emitters functionalized with fluorine and benzyl sulfonyl electron withdrawing substituents on phenylpyridine ligands, demonstrating the possibility to finely tune the emission color of the complexes by properly selecting the position of substituents and the number of fluorine atoms.[71] A green OLED fabricated with $(2F\text{-sulf-ppy})_2Ir(acac)$ (Figure 7) showed enhanced luminous efficiency (LE up to 24.2 cd/A) versus the reference device made with the non-functionalized $(ppy)_2Ir(acac)$ complex, as a possible consequence of both the steric effect of the bulky benzylsulfonyl groups in the ligands and the enhanced electron mobility induced by the fluorine atoms.[72] We also recently synthesized an heteroleptic blue-green emitting iridium complex with perfluorinated phenylpiridine and pyridinetriazole ligands (Ir-F19 in Figure 7),[73] displaying intense photoluminescence. Good color rendering index (CRI=76), CIE coordinates (0.43, 0.42) and luminous efficiency of 10.1 cd/A up to 1000 cd/$m^2$ were recorded for white light emitting devices (WOLEDs) with a rather simple architecture based on two stacked layers of the blue-green Ir-F19 and the orange $Ir(MDQ)_2(acac)$ complexes.

Fluorinated benzimidazole-based iridium complexes (1F-Ir, 2F-Ir and 3F-Ir in Figure 7) with strong bluish green emission and high quantum yields (68-81%) have been recently reported by Zhao *et al.* and used for the fabrication of OLEDs with simple configuration and high current efficiencies (58.9 cd/A for 2F-Ir based device) even at high luminance of 5000 cd/$m^2$, these being greatly improved versus the performances of a reference device based on the non-fluorinated iridium complex analogue.[74] A significant improvement of device's efficiency (60.3 cd/A and 47.3 lm/W), that is one of the highest ever reported for yellow/orange phosphorescent OLEDs, was also found by Lv *et al.* when using the stable yellow $[(tfbt)_2Ir(acac)]$ emitter (Figure 7) rather than the corresponding $(bt)_2Ir(acac)$ reference complex without fluorine substituents.[75]

The blue FK306 iridium emitter with fluorinated bipyridyl ligands was found to have high photoluminescence quantum yield (78%) in thin mCP (*N,N*-dicarbazolyl-3,5-benzene) host film and to be suitable as pure blue phosphor for OLEDs, reaching power efficiency of over 30 lm/W.[76]

Various fluorinated cationic iridium complexes were also developed for application in both OLEDs and light emitting electrochemical cells (LEECs).[77] Blue-green LEECs and OLEDs were fabricated by He *et al.* using cationic iridium complexes (**1-3** in Figure 7) with a gradually fluorinated phenyl group bound to pyrazolylpyridine ligand.[77a] Increasing the number of fluorine atoms, a decrease of the efficiency and stability of LEECs was observed, due to a decrease of the complexes' electrochemical stability, despite the fact that intramolecular π-π stacking interactions are increased. Fluorination was also found by the same authors to enhance the electron-trapping ability of the complexes and to blue shift their electroluminescence in OLEDs.[77a] Pal *et al.* recently reported that the functionalization with trifluoromethyl, trifluoromethoxy, trifluoromethylthiosulfonyl electron withdrawing groups in the phenylpyridine ligands of the $(ppy)_2Ir(dtBubpy)^+ PF_6^-$ emitter leads to a blue shift of the complex photoluminescence and moderate (up to 8.9 Cd/A and 4.4 lm/W) external quantum efficiencies were found for the fluorinated complexes-based LEECs.[77b]

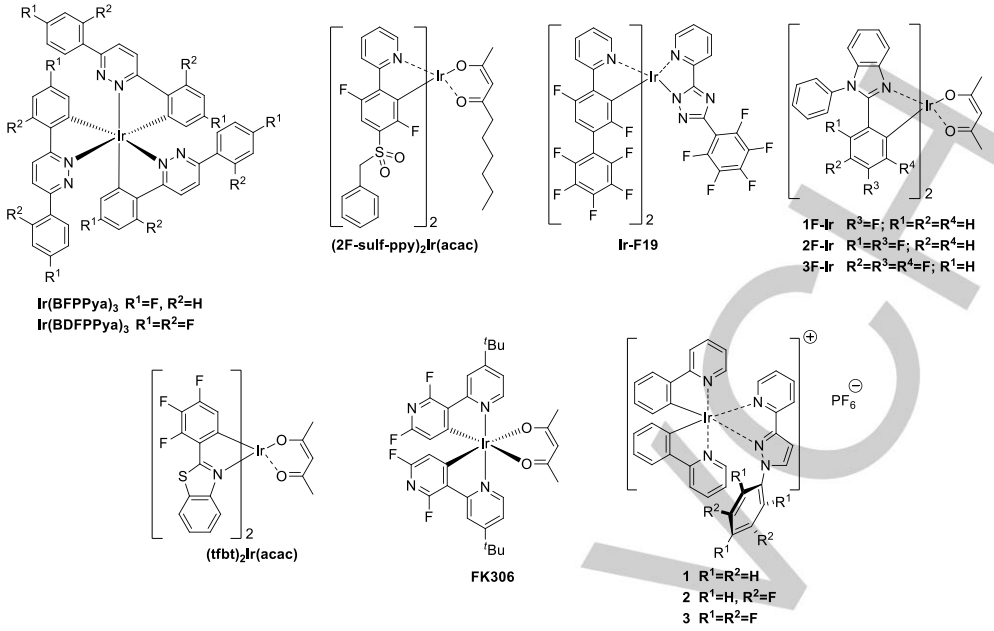


**Figure 7.** Iridium complexes for OLEDs

A series of cationic Ir(dfppy)$_2$(pzpy) complexes (dfppy: 2,4-difluorophenylpyridine and pzpy:pyrazolylpyridine) differing in the nature of the fluorinated counterion (tetrafluoroborate, hexafluorophosphate, 4-fluorophenylborate, pentafluorophenylborate) was also reported by Ma *et al.* and the anionic influence on light emitting device performances was investigated. [78] In this case, increasing the steric hindrance of the fluorinated counterion, a significant reduction of ionic interactions and molecular aggregation in the solid state occurs, this leading to (*i*) an improvement of the photoluminescence efficiency of complexes, (*ii*) a reduction of the anionic drift under the working bias in OLEDs and (*iii*) an electroluminescence blue shift to only 452 nm for deep-blue-light emitting devices. This is among the shortest emission wavelengths recorded for ionic transition metal complexes based devices.

Dinuclear iridium complexes with fluorinated ligands were developed mainly for applications as single emitters in white OLEDs.[79] For instance, He *et al.* synthesized the (dfppy)$_4$Ir$_2$(dipic-FL) dimer with an acceptor-donor-acceptor (A-D-A) framework, in which two iridium complex peripheral moieties bearing dfppy [2-(2,4-difluorophenyl)pyridine] and picolinate ligands are connected *via* a 9,9-dioctyl-9H-fluorene bridge (Figure 8).[79b] The white broad electroluminescence of the dimer used as single emitter in WOLED was attributed to the combination of intense short wavelength peaks (at 473 and 540 nm) resulting from the intrinsic emission of (dfppy)$_2$Ir(pic) moieties and a weak long-wavelength emission band (at 580-660 nm) due to an intramolecular charge transfer transition between the central bridge and the side phosphors.

Dinuclear complexes with A-D-A type structure bearing pheripheral fluorinated platinum(II) phosphors and a central bridging core were used as single emitters in white OLEDs as well. For example, dimers with two side (dfppy)Pt(pic) complexes bound to 4,4'-bis(oxyhexyloxy)-biphenyl or bis(hexyloxy)triphenylamine-substituted indolo[3,2-*b*]carbazole cores were reported by the groups of Wang[80] and Yu, [81] respectively [see structures of (dfppy)$_2$Pt(dipic) and (dfppy)$_2$Pt$_2$(dipic-BTICz) in Figure 8]. In both cases, the conjugated unit of the central bridge enhances the dimer carrier-transporting ability and the blue photoluminescence of side platinum complexes, whereas the non-conjugated alkyl chains in the bridge allow to control intra- and inter-molecular energy transfer processes responsible for the red emission of excimers that result from aggregation in the solid state. As a consequence, stable white electroluminescence was observed for OLEDs made with these emitting dimers.

Few examples of new fluorinated complexes of transition metals different from iridium and platinum have been also reported in the last decade for OLEDs applications. Among them, a novel Er(III) fluorinated β-diketonate ternary complex [Er(tfnb)$_3$(bipy) in Figure 9] was used by Martín-Ramos *et al.* as near infrared emitter in a full solution-processed NIR-OLED.[82] In this case, fluorination does not modify the energy of triplet levels of the β-diketonate ligand, hence it does not affect the resonant transfer from the ligand to the NIR emitting lanthanide ion. The beneficial effect of fluorine atoms consists, instead, in reducing the energy of C-F oscillators versus that of C-H bonds, this resulting in the reduction of non-radiative losses of the lanthanide ion emission.

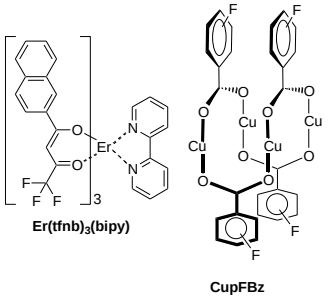


**Figure 9.** Erbium and copper complexes for OLEDs

Another worth noting study, although dealing with transition metal salts with charge transport properties rather than light emitting complexes, was reported in 2014 by Schmid *et al.* about the use of fluorinated copper(I) carboxylates as very efficient p-

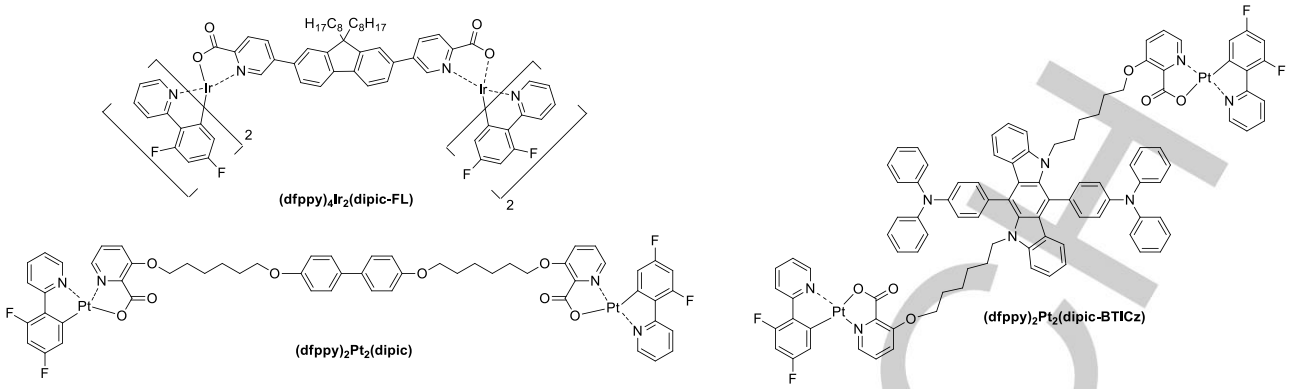


**Figure 8.** Dinuclear Iridium and platinum complexes for OLEDs

dopants for hole transporting layers in white OLEDs.[83] In particular, fluorinated copper benzoates (CupFBz in Figure 9) were found to have excellent electrical conductivity and optical transparency when doped into a triarylamine α-NPD hole conducting layer. Moreover, increasing the fluorination degree of benzoate units, an increase of current density was observed, due to the increase of Lewis acidity of the copper centers that enhances the strength of the donor-acceptor interactions with the host molecules.

## 6. Conclusions

The state of art in the development of organic-based electronics evidences that various levels of maturity have been reached for the most used devices.

OLED technology appears to be the most advanced technology platform. OLED and AMOLED (Active Matrix Organic Light Emitting Diodes) displays are nowadays present in many devices such as cellular phones and large area color TV screens. For these applications both polymers and small molecules have been employed, but the use of phosphorescent organometallic complexes has enabled to reach the best performances. In OLED technology the blue emission was a target relatively hard to achieve, and the fluorination strategy revealed to be one of the most effective in shifting the emission of these complexes towards shorter wavelength, reaching a deep blue electroluminescence.

Presently, the OSCs technology is continuously growing and complex molecular architectures both in polymeric materials and small molecules have been devised for driving the PCE of organic solar cells to values comparable with those of conventional silicon-based devices. The development of D-A polymers and small molecules characterized by low band-gaps has boosted this trend and the role played by fluorine functionalization is of paramount prominence. Fluorination is effective in improving the PCE, acting both on the HOMO/LUMO levels and on the solid-state supramolecular organization in the active thin film of devices. However, the positive effect of introducing fluorine atoms in the D-A structure of these materials, is the result of an appropriate choice of the position in the conjugated system. Some examples reported in this review evidence that a negative effect on the PCE is sometimes measured, since the position of fluorine atoms reduces the aggregation abilities of the active material in the thin film, with a detrimental effect on charge separation and transport. Further improvement of BHJ OSCs performances has been achieved with the introduction of non-fullerene acceptors (NFAs). In fact, the highest PCE reported so far has been obtained combining D-A polymers and NFA both bearing fluorine substituents in appropriate positions.

OFET technology is also emerging and it benefits from the introduction of D-A polymer and small molecules. Considering that these materials generally display p-type mobilities, the main target of fluorine functionalization in the OFET applications is to attain efficient n-type charge transport and a balanced ambipolar behavior, that is a critical feature for complementary metal-oxide-semiconductor devices (CMOSs), largely used in logic circuits. The fluorination approach allowed to achieve meaningful results in this field owing to the electronic effects of fluorine on the frontier orbital levels but also in promoting a solid-state crystalline structure able to grant an effective electron transport.

In conclusion, fluorination still shows strong impact for driving the performances of organic semiconductors to comparable or higher level with respect to the silicon conventional counterparts and to make the “plastic electronics” an important technology of the next future.

**Keywords:** Fluorine • Organic field effect transistors • Organic light emitting diodes • Solar cells • Organic semiconductors

[1] F. Babudri, G. M. Farinola, F. Naso, R. Ragni *Chem. Commun*. **2007**, 1003-1022.

[2] a) A. Punzi, D. I. Coppi, S. Matera, M. A. M. Capozzi, A. Operamolla, R. Ragni, F. Babudri, G. M. Farinola *Org. Lett.* **2017**, *19*, 4754-4757; b) F. Babudri, A. Cardone, C. T. Cioffi, G. M. Farinola, F. Naso, R. Ragni *Synthesis* **2006**, *8*, 1325-1332; c) R. Ancora, F. Babudri, G. M. Farinola, F. Naso, R. Ragni *Eur. J. Org. Chem.* **2002**, *24*, 4127-4130; d) A. Operamolla, R. Ragni, O. H. Omar, G. Iacobellis, A. Cardone, F. Babudri, G. M. Farinola *Curr. Org. Synth.* **2012**, *9*, 764-778; e) M. Ambrico, P. F. Ambrico, A. Cardone, N. F. Della Vecchia, T. Ligonzo, S. R. Cicco, T. M. Talamo, A. Napolitano, V. Augelli, G. M. Farinola, M. d'Ischia *J. Mater. Chem. C* **2013**, *1*, 1018-1028; f) M. Ambrico, P. F. Ambrico, A. Cardone, T. Ligonzo, S. R. Cicco, R. Di Mundo, V. Augelli, G. M. Farinola, *Adv. Mater.* **2011**,*23*, 3332; g) M. C. Tanese, G. M. Farinola, B. Pignataro, L. Valli, L. Giotta, S. Conoci, P. Lang, D. Colangiuli, F. Babudri, F. Naso, L. Sabbatini, P. G. Zambonin, L. Torsi, *Chem Mater.* **2006**, *18*, 778-784; h) D. Pisignano, L. Persano, R. Cingolani, G. Gigli, F. Babudri, G. M. Farinola, F. Naso *Appl. Phys. Lett.* **2004**, *84*, 1365-1367; i) G. Marzano, D. Kotowski, F. Babudri, R. Musio, A. Pellegrino, S. Luzzati, R. Po, G. M. Farinola *Macromolecules* **2015**, *48*, 7039-7048; l) G. Marzano, F. Carulli, F. Babudri, A. Pellegrino, R. Po, S. Luzzati, G. M. Farinola *J. Mater. Chem. A* **2016**, *4*, 17163-17170.

[3] For OSCs see: S. Günes, H. Neugebauer, N. S. Sariciftci Chem. Rev. **2007,** 107, 1324–1338; for OFETs see: a) L. Torsi, A. Dodabalapur *Anal. Chem.*, **2005**, 77, 380 A–387 A; b) A. Operamolla, G. M. Farinola *Eur. J. Org. Chem.* **2011**, 423-450; for OLEDs see S.R. Forrest, D.C.D. Bradley, M. E. Thompson *Adv. Mater.* **2003**, *15*, 1043-1048.

[4] G. Yu, J. Gao, J.C. Hummelen, F. Wudl, A.J. Heeger *Science* **1995**, *270*, 1789-1791.

[5] Y. Liang, L. Yu *Macromolecules* **2012**, *45*, 607-632.

[6] a) F. Meyer *Progr. Polym. Sci.* **2015**, *47*,70-91; b) N. Leclerc, P. Chávez, O. A. Ibraikulov , T. Heiser 2, P. Lévêque *Polymer* **2016**, *8*, 11; c) X-P. Xu, Y. Li, M-M. Luo, Q. Peng *Chin. Chem. Lett.* **2016**, *27,* 1241-1249; d) Q. Zhang,M. Allison Kelly,N. Bauer,Wei You *Acc. Chem. Res*. **2017**, *50*, 2401−2409.

[7] Z. Li, T. Zhang, Y. Xin, X. Zhao, D. Yang, F. Wu X. Yang *J. Mater. Chem. A***, 2016**, *4*, 18598-18606.

[8] Z. Cong, S. Liu, B. Zhao, W. Wang, H. Liu, J. Su, Z. Guo, W. Wei, C Gao, Z. An *RSC Advances* **2016**, *6,* 77525-77534.

[9] Q. Zhang,L. Yan, X. Jiao, Z. Peng, S. Liu, J. J. Rech, E. Klump, H. Ade, F. So, W. You *Chem. Mater*. **2017**, *29*, 5990-6002.

[10] N. Bauer, Q. Zhang, J. Zhu, Z. Peng, L. Yan, C. Zhu, H. Ade, X. Zhan, Wei You *J. Mater. Chem. A***, 2017**, *5*, 22536-22541.

[11] M. Cai, X. Bao, Y. Fang Liu, C. Li, X. Wang, Z. Lan, R. Yang, X. Wan *Chem. Mater*. **2017**, *29*, 9162-9170.

[12] Y. Li, J. Wang, Y. Liu, M. Qiu, S. Wen, X. Bao, N. Wang, M. Sun, R. Yang *ACS Appl. Mater. Interfaces* **2016**, *8*, 26152-26161.

[13] J. Yuan, M. J. Ford, Y. Zhang, H. Dong, Z. Li, Y. Li, T.-Q. Nguyen, G. C. Bazan, W. Ma *Chem. Mater.* **2017**, *29*, 1758-1768.

[14] B. He, Q. Yin, X. Yang, L. Liu, X. –F. Jiang, J. Zhang, F. Huang, Y. Cao *J. Mat. Chem. C***2017**, *5*, 8774-8781.

[15] a) A. Cardone, C. Martinelli, M. Losurdo, E. Dilonardo, G. Bruno, G. Scavia, S. Destri, P. Cosma, L. Salamandra, A. Reale, A. Di Carlo, A. Aguirre, B. Milián-Medina, J. Gierschner, G. M. Farinola *J. Mater. Chem. A* **2013**, *1*, 715-727; b) E. Dilonardo, A. Cardone, C. Martinelli, M. M. Giangregorio, M. Losurdo, P. Capezzuto, G. M. Farinola, F. Babudri, F. Naso, G. Bruno *Synth. Met*. **2012**, *161,* 2607-2611.

[16] J. Shin, M. Kim, J. Lee, H. Gyu Kim, H. Hwang, K. Cho *Chem. Commun*. **2017**, *53*, 1176-1179.

[17] Z. Cong, H. Liu, W. Wang, J. Liu, B. Zhao, Z. Guo, C. Gao, Z. An *Dyes Pigments* **2017**,*146* 529-536.

[18] Z. Zhao, Y. Zhang, Y. Wang, X. Qin, J. Wu, J. Hou *Org. Electron.* **2016**, *28*, 178-183.

[19] W. Zhao, S. Li, H. Yao, S. Zhang, Y. Zhang, B. Yang, J. Hou *J. Am. Chem. Soc*. **2017**, *139*, 7148−7151.

[20] S. Guo, J. Ning , V. Körstgens, Y. Yao, E. M. Herzig, S. V. Roth, P. Müller-Buschbaum *Adv. Energy Mater*. **2015**, *5*, 1401315.

[21] J. Kim, J. Baek Park, W.-H. Lee, J.-H. Kim, D.-H. Hwang, I.-N. Kang *Journal of Polymer Science, Part A: Polymer Chemistry* **2017**, *55*, 2506–2512.

[22] a) Y. Lin, Y. Li, X. Zhan *Chem. Soc. Rev* **2012**, *41*, 4245-4272; b) J. E. Coughlin, Z. B. Henson, G. C. Welch, G. C. Bazan *Acc. Chem. Res.* **2014**, *47*, 257–270; c) Y. Lin, X. Zhan, *Acc. Chem. Res.* **2016**, *49*, 175−183.

[23] S. Furukawa, H. Komiyama, T. Yasuda *J. Phys. Chem. C* **2016**, *120*, 21235-21241.

[24] B. Qiu, J. Yuan, X. Xiao, D. He, L. Qiu, Y. Zou, Z.-G. Zhang, Y. Li *ACS Appl. Mater. Interfaces* **2015**, *7*, 25237-25246.

[25] J.-L. Wang, K.-K. Liu, S. Liu, F. Xiao, Z.-F. Chang, Y.-Q. Zheng, J.-Hu Dou, R.-B. Zhang, H.-B. Wu, J. Pei, Y. Cao *Chem. Mater.* **2017**, *29*, 1036-1046.

[26] C. B. Nielsen, S. Holliday, H.-Y. Chen, S. J. Cryer, I. McCulloch, *Acc. Chem. Res*. **2015**, *48*, 2803−2812.

[27] W. Zhao, S. Li, H. Yao, S. Zhang, Y. Zhang, B. Yang, J. Hou, *J. Am. Chem. Soc.* **2017**, *139*, 7148−7151.

[28] L. Zhao, H. Sun, X. Liu, C. Liu, H. Shan, J. Xia, Z. Xu, F. Chen, Z.-K. Chen, W. Huang *Chem. Asian J.* **2017**, *12*, 2052-2056.

[29] a) S. M. Yoon, S. J. Lou, S. Loser,J. Smith, L. X. Chen, A. Facchetti, T. Marks, *Nano Lett.* **2012**, *12*, 6315-6321; b) Y. Kuzumoto, H. Matsuyama, M. Kitamura, *Jpn. J. of Appl. Phys.* **2014**, *53*, 04ER16-1-5.

[30] a) J. L. Yang , S. Schumann , R. A. Hatton , T. S. Jones, *Org. Electron.* **2010** , *11* , 1399-1402; b) H. Peisert , M. Knupfer , T. Schwieger , G. G. Fuentes , D. Olligs, J. Fink , Th. Schmidt *J. Appl. Phys.* **2003** , *93* , 9683-9692.

[31] B. Verreet, B. P. Rand, D. Cheyns, A. Hadipour, T. Aernouts, P. Heremans, A. Medina, C. G. Claessens, T. Torres *Adv. Energy Mater.* **2011**, *1*, 565–568.

[32] F. S. Etheridge, R. J. Fernando, S. Pejić, M. Zeller, G. Sauvé *Beilstein J. Org. Chem.* **2016**, *12*, 1925-1938.

[33] a) Tsumura, A.; Koezuka, H.; Ando, T. *Appl. Phys. Lett.* **1986**, *49*, 1210-1212; b) Horowitz, G. *Adv. Mater.* **1998**, *10*, 365-377; c) Dimitrakopoulos, C. D.; Malenfant, P. R. L. *Adv. Mater.* **2002**, *14*, 99-117.

[34] C. Wang, H. Dong, W. Hu, Y. Liu, D. Zhu, *Chem. Rev.* **2012**, *112*, 2208-2267.

[35] J. Zaumseil, H. Sirringhaus *Chem. Rev.* **2007**, *107*,1296-1323.

[36] P. Li, L. Xu, H. Shen, X. Duan, J. Zhang, Z. Wei, Z. Yi, C. Di, S. Wang, *ACS Appl. Mater. Interfaces* **2016**, *8*, 8620-8626.

[37] T. Bura, S. Beaupré, O. A. Ibraikulov, M.-A. Légaré, J. Quinn, P. Lévêque, T. Heiser, Y. Li, N. Leclerc, M. Leclerc *Macromolecules* **2017**, *50*, 7080-7090.

[38] G. Dansoa Tabi, B. Nketia-Yawson, J. Young Lee, K. Cho, B. Lim, Y.-Y. Noh *RSC Adv.***2017**, *7*, 1110-1117.

[39] T.Lei, X. Xia, J.-Y. Wang, C.-J. Liu, J. Pei, *J. Am. Chem. Soc.* **2014**, *136*, 2135−2141.

[40] Z. Fei, P. Boufflet, S. Wood,J. Wade, J. Moriarty, E. Gann, E. L. Ratcliff, C. R. McNeill, H. Sirringhaus, J.-S. Kim, M. Heeney, *J. Am. Chem. Soc.* **2015**, *137*, 6866-6879.

[41] J. T. Blaskovits, T. Bura, S. Beaupré, S. A. Lopez, C. Roy, J. de Goes Soares, A. Oh, J. Quinn, Y. Li, A. Aspuru-Guzik, M. Leclerc, *Macromolecules* **2017**, *50*, 162-174.

[42] P. Boufflet, Y. Han, Z. Fei, N. D. Treat, R.Li, D.-M. Smilgies, N. Stingelin, T. D. Anthopoulos, M. Heeney *Adv. Funct. Mater*. **2015**, *25*, 7038-7048.

[43] K. Miao, G. J. Chae, X. Wu, Q. Shu, X. Zu, B. Sun, J. Fan, S. Cho *RSC Adv.* **2016**, *6*, 29164-29171.

[44] B. Nketia-Yawson, H.-S. Lee, D. Seo, Y. Yoon, W.-T. Park, K. Kwak, H. Jung Son, B. Kim, Y.-Y. Noh *Adv. Mater.* **2015**, *27*, 3045–3052.

[45] R. Sato, M. Dogishi, T. Higashino, T. Kadoya, T. Kawamoto, T. Mori *J. Phys. Chem. C* **2017**, *121*, 6561−6568.

[46] Shukla, D. Nelson, S. F., Freeman, D. C., Rajeswaran, M., Ahearn, W. G., Meyer, D. M., Carey, J. T., *Chem. Mater*. **2008**, *20*, 7486-7491.

[47] Yuan,Y. Ma,T. Geßner, M. Li, L. Chen, M. Eustachi, R. T. Weitz, C. Li, K. Müllen *Org. Lett.* **2016**, *18*, 456-459.

[48] J. S. Reddy, T. Kale, G. Balaji, A. Chandrasekaran, S. Thayumanavan *J. Phys. Chem. Lett*. **2011**, *2*, 648-654.

[49] Z. Liang, Q. Tang, J. Liu, J. Li, F. Yan, Q. Miao *Chem. Mater.* **2010**, *22*, 6438–6443.

[50] a) J. Zhoua, Y. Jiang, Z. Wang, S. Hu, P. Gan, X. Shen *Eur. Phys. J.-Appl. Phys.* **2016**, *73(2)*, 20201/1-20201/6; b) X. Luo, L. Du, B. Yao, W. Lv, L. Sun, Y. Li, Z. Wu, Z. Wen, Y. Peng *J. Mater. Chem.*

*C: Materials for Optical and Electronic Devices* **2015**, *3(28)*, 7336-7344.

[51] H. Jiang, J. Ye, P. Hu, F. Wei, K. Du, N. Wang, T. Ba, S. Feng, C. Kloc *Scientific Reports* **2014**, *4*, 7573.

[52] X. Shao, S. Wang, X. Li, Z. Su, Y. Chen, Y. Xiao *Dyes Pigments* **2016**,*132*, 378-386.

[53] a) F. Babudri, A. Cardone, G. M. Farinola, C. Martinelli, R. Mendichi, F. Naso, M. Striccoli, *Eur. J. Org. Chem.* **2008**, 1977-1982; b) A. Cardone, C. Martinelli, V. Pinto, F. Babudri, M. Losurdo, G. Bruno, P. Cosma, F. Naso, G.M. Farinola, *J. Polym. Sci. Pol. Chem.* **2010**, *48*, 285-291; c) G. M. Farinola, A. Cardone, F. Babudri, C. Martinelli, F. Naso, G. Bruno, M. Losurdo, *Materials* **2010**, *3*, 3077-3091; d) A. Cardone, C. Martinelli, F. Babudri, F. Naso, V. Pinto, G. M. Farinola, *Curr. Org. Synth.* **2012**, *9*, 150-162; e) G. M. Farinola, F. Babudri, A. Cardone, O. Hassan Omar, C. Martinelli, F. Naso, V. Pinto, R. Ragni, *Advances in Science and Technology* **2010**, *75*, 108-117.

[54] a) M. Burger, F. Floris, A. Cardone, G.M. Farinola, V. Morandi, F. Marabelli, D. Comoretto, *Org. Electron.* **2017**, *43*, 214-221; b) M. Piacenza, F. Della Sala, G. M. Farinola, C. Martinelli, G. Gigli, *J. Phys. Chem. B* **2008**, *112*, 2996-3004; c) M. Piacenza, D. Comoretto, M. Burger, V. Morandi, F. Marabelli, C. Martinelli, G.M. Farinola, A. Cardone, G. Gigli, F. Della Sala, *ChemPhysChem* **2009**, *10*, 1284-1290; d) M. Losurdo, M. M. Giangregorio, P. Capezzuto, A. Cardone, C. Martinelli, G. M. Farinola, F. Babudri, F. Naso, M. Büchel, G. Bruno, *Adv. Mater.* **2009**, *21*, 1115-112.

[55] R. Milad, J.Q. Shi, A. Aguirre, A.Cardone, B. Milian-Medina, G. M. Farinola, M. Abderrabba, J. Gierschner, *J. Mater. Chem. C* **2016**, *4*, 6900-6906.

[56] M. Losurdo, M. M. Giangregorio, P. Capezzuto, G. Bruno, F. Babudri, A. Cardone, C. Martinelli, G. M. Farinola, F. Naso, M. Büchel, *Polymer* **2008**, *49*, 4133-4140.

[57] H. H. Fong, J.-K. Lee, Y.-F. Lim, A. A. Zakhidov, W. W. H. Wong, A. B. Holmes, C. K. Ober, G. G. Malliaras *Adv. Mater.* **2011**, *23*, 735-739.

[58] W. Zhong, J. Liang, S. Hu, X.-F. Jiang, L. Ying, F. Huang, W. Yang, Y. Cao *Macromolecules* **2016**, *49*, 5806-5816.

[59] Y. Mizuno, I. Takasu, S. Uchikoga, S. Enomoto, T. Sawabe, A. Amano, A. Wada, T. Sugizaki, J. Yoshida, T. Ono, C. Adachi, *J. Phys. Chem. C* **2012**, *116*, 20681-20687.

[60] W. Lu, J. Kuwabara, T. Iijima, H. Higashimura, H. Hayashi, T. Kanbara *Macromolecules* **2012**, *45*, 4128−4133.

[61] Z. Li, Z. Wu, W. Fu, P. Liu, B. Jiao, D. Wang, G. Zhou, X. Hou, *J. Phys. Chem. C* **2012**, *116*, 20504-20512.

[62] D. Liu, H. Ren, J. Li, Q. Tao, Z. Gao, *Chem. Phys. Lett.* **2009**, *482*, 72-76.

[63] Y.-J. Yu, O. Solomeshch, H. Chechik, A. A. Goryunkov, R. F. Tuktarov, D. H. Choi, J.-I. Jin, Y. Eichen, N. Tessler, *J. Appl. Phys.* **2008**, *104*, 124505-1-3.

[64] B. Milián-Medina, S. Varghese, R. Ragni, H. Boerner, E. Ortí, G. M. Farinola, J. Gierschner *J. Chem. Phys.* **2011**, *135*, 124509-1-6.

[65] a) F. Babudri, A. Cardone, L. De Cola, G. M. Farinola, G. S. Kottas, C. Martinelli, F. Naso, *Synthesis* **2008**, *10*, 1580-1588; b) C. Martinelli, G. M. Farinola, V. Pinto and A. Cardone, *Materials* **2013**, *6*, 1205-1236; c) F. Babudri, G. M. Farinola, F. Naso, R. Ragni, G. Spina, *Synthesis* **2007**, *19*, 3088-3092.

[66] a) H. Bi, K. Ye, Y. Zhao, Y. Yang, Y. Liu, Y. Wang, *Org. Electron.* **2010**, *11*, 1180-1184; b) F. Babudri, D. De Palma, G. M. Farinola, R. Ragni, F. Naso, *Synthesis* **2008**, *8*, 1227-1232.

[67] T. Kamata, H. Sasabe, Y. Watanabe, D. Yokoyama, H. Katagiri, J. Kido *J. Mater. Chem. C* **2016**, *4*, 1104-1110.

[68] C. Si, Z. Li, K. Guo, X. Lv, S. Pan, G. Chen, Y. Hao, B. Wei *Dyes Pigments* **2018**, *148*, 329-340.

[69] Z. Li, B. Jiao, Z. Wu, P. Liu, L. Ma, X. Lei, D. Wang, G. Zhou, H. Hud, X. Hou, *J. Mater. Chem. C* **2013**, *1*, 2183-2192.

[70] C. Liu, L. Mao, H. Jia, Z. Liao, H. Wang, B. Mi, Z. Gao, *Sci. China Chem.* **2015**, *58*, 640-649.

[71] R. Ragni, E. Orselli, G. S. Kottas, O. Hassan Omar, F. Babudri, A. Pedone, F. Naso, G. M. Farinola, L. De Cola, *Chem. Eur. J.* **2009**, *15*, 136-148.

[72] W. Mróz, R. Ragni, F. Galeotti, E. Mesto, C. Botta, L. De Cola, G.M. Farinola, U. Giovanella, *J. Mater. Chem. C* **2015**, *3*, 7506-7512.

[73] R. Ragni, V. Maiorano, M. Pugliese, A. Maggiore, E. Orselli, F. Babudri, G. Gigli, L. De Cola, G. M. Farinola, *Synth. Met.* **2017**, *227*, 148-155.

[74] J.-H. Zhao, Y.-X. Hu, Y. Dong, X. Xia, H.-J. Chi, G.-Y. Xiao, X. Li, D.-Y. Zhang *New J. Chem.* **2017**, *41*, 1973-1979.

[75] Y.-L. Lv, Y.-X. Hu, J.-H. Zhao, G.-W. Zhao, Y. Qi, X. Li, H.-J. Chi, Y. Dong, G.-Y. Xiao, Z.-S. Su, *Opt.l Mater.* **2015**, *49*, 286-291

[76] F. Kessler,Y. Watanabe, H. Sasabe, H. Katagiri, M. K. Nazeeruddin, M. Grätzel, J. Kido, *J. Mater. Chem. C* **2013**, *1*,1070-1075.

[77] a) L. He, L. Duan, J. Qiao, D. Zhang, G. Dong, L. Wang, Y. Qiu, *Synthetic Met.* **2013**, *166*, 52- 56; b) A. K. Pal, D. B. Cordes, A. M. Z. Slawin, C. Momblona, E. Ortı, I. D. W. Samuel, H. J. Bolink, E. Zysman-Colman, *Inorg. Chem.* **2016**, *55*, 10361−10376; c) C. D. Sunesh, K. Shanmugasundaram, M. S. Subeesh, R. K. Chitumalla, J. Jang, Y. Choe, *ACS Appl. Mater. Interfaces* **2015**, *7*, 7741-7751; d) L. Skórka, M. Filapek, L. Zur, J. G. Małecki, W. Pisarski, M. Olejnik, W. Danikiewicz, S. Krompiec, *J. Phys. Chem. C* **2016**, *120*, 7284−7294; e) C. D. Sunesh, G. Mathai, Y.-R. Cho, Y. Choe, *Polyhedron* **2013**, *57*, 77-82.

[78] D. Ma, C. Zhang, Y. Qiu, L. Duan, *Org. Electron.* **2016**, *39*, 16-24.

[79] a) Z. Hao, H. Jiang, Y. Liu, Y. Zhang, J. Yu, Y. Wang, H. Tan, S. Su, W. Zhu, *Tetrahedron* **2016**, *72*, 8542-8549; b) K. He, X. Wang, J. Yu, H. Jiang, G. Xie, H. Tan, Y. Liu, D. Ma, Y. Wang, W. Zhu, *Org. Electron.* **2014**, *15*, 2942-2949.

[80] a) Y. Wang, X. Deng, Y. Liu, M. Ni, M. Liu, H. Tan, X. Li, W. Zhu, Y. Cao, *Tetrahedron* **2011**, *67*, 2118-2124; b) Y. Wang, J. Luo, Y. Liu, Z. Zhang, H. Tan, J. Yu, G. Lei, M. Zhu, W. Zhu, *Org. Electron.* **2012**, 13, 1646-1653.

[81] J. Yu, J. Luo, Q. Chen, K. He, F. Meng, X. Deng, Y. Wang, H. Tan, H. Jiang, W. Zhu, *Tetrahedron* **2014**, *70*, 1246-1251.

[82] P. Martín-Ramos,C. Coya, Á. L. Álvarez,M. Ramos Silva, C. Zaldo, J.A. Paixão, P. Chamorro-Posada, J. Martín-Gil, *J. Phys. Chem. C* **2013**, *117*, 10020-10030.

[83] G. Schmid, J. H. Wemken, A. Maltenberger, C. Diez, A. Jaeger, T. Dobbertin, O. Hietsoi, C. Dubceac, M. A. Petrukhina *Adv. Mater.* **2014**, *26*, 878-885.

MICROREVIEW

Recent progresses on fluorinated conjugated polymers, small molecules and organometallic complexes as organic semiconductors in electronic devices such as OSCs, OFETs and OLEDs are reviewed.

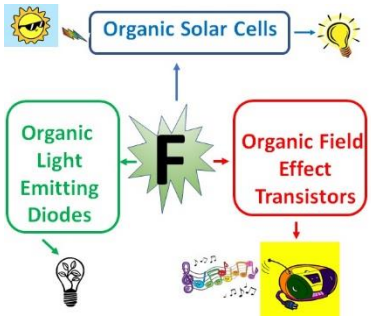


**Organofluorine semiconductors**

*Roberta Ragni, Angela Punzi, Francesco Babudri* and Gianluca Maria Farinola**

***Page No. – Page No.***

**Organic and organometallic fluorinated materials for electronics and optoelectronics: a survey on recent research**